Proc Indian Natn Sci Acad, **70, A,** No. 1, January 2004, pp.95–122
© Printed in India.

ONE YEAR OF EVIDENCE FOR NEUTRINOLESS DOUBLE BETA DECAY

H V KLAPDOR-KLEINGROTHAUS
Spokesman of the HEIDELBERG-MOSCOW and GENIUS Collaborations,
Max-Planck-Institut für Kernphysik, P.O. 10 39 80,
D-69029 Heidelberg (Germany)

(Received 10 January 2003; Accepted 30 June 2003)

The present experimental status in the search for neutrinoless double beta decay is reviewed, with emphasis on the first indication for neutrinoless double beta decay found in the HEIDELBERG-MOSCOW experiment, giving first evidence for lepton number violation and a Majorana nature of the neutrinos. Future perspectives of the field are briefly outlined.

Key Words: Heidelberg-Moscow Experiment; Lepton Number Violation; Majorana Neutrino; Double Beta Decay of Germanium

1 Introduction

The neutrino oscillation interpretation of the atmospheric and solar neutrino data deliver a strong indication for a non-vanishing neutrino mass. While such kind of experiments yield information on the difference of squared neutrino mass eigenvalues and on mixing angles (for the present status see, e.g. refs.[1-4], the absolute scale of the neutrino mass is still unknown. Information from double beta decay experiments is indispensable to solve these questions[5-7]. Another even more important problem is that of the fundamental character of the neutrino, whether it is a Dirac or a Majorana particle[8,9]. Neutrinoless double beta decay could also answer this question. Perhaps the main question, which can be investigated by double beta decay with highest sensitivity, is that of lepton number conservation or non-conservation.

Double beta decay, the rarest known nuclear decay process, can occur in different modes:

$2\nu\beta\beta$ – decay :

$$A(Z,N) \rightarrow A(Z+2,N-2) + 2e^- + 2\bar{\nu}_e \qquad \ldots(1)$$

$0\nu\beta\beta$ – decay :

$$A(Z,N) \rightarrow A(Z+2,N-2) + 2e^- \qquad \ldots(2)$$

$0\nu(2)\chi\beta\beta$ – decay :

$$A(Z,N) \rightarrow A(Z+2,N-2) + 2e^- + \chi \qquad \ldots(3)$$

While the two-neutrino mode (1) is allowed by the Standard Model of particle physics, the neutrinoless mode ($0\nu\beta\beta$) (2) requires violation of lepton number ($\Delta L=2$). This mode is possible only if the neutrino is a Majorana particle, i.e., the neutrino is its own antiparticle (E. Majorana[8], G. Racah[9], for subsequent works we refer to refs.[10-12], for some reviews see refs.[7,13-16]. First calculations of $0\nu\beta\beta$ decay based on the Majorana theory have been done by W.H. Furry[17]. The most general Lorentz-invariant parametrization of neutrinoless double beta decay is shown in Fig.1.

The usually used assumption is that the first term (i.e. the Majorana mass mechanism) dominates the decay process. However, as can be seen from Fig.1, and as discussed elsewhere (see refs.[7,19-21]) neutrinoless double beta decay can not only probe a Majorana neutrino mass, but various new physics scenarios beyond the Standard Model, such as R-parity violating supersymmetric models, R-parity conserving SUSY models, leptoquarks, violation of Lorentz-invariance, and compositeness (for a review see refs.[7,19-20]). Any theory containing lepton number violating interactions can in principle lead to this process allowing to obtain information on the specific underlying theory. It has been pointed out already in 1982, however, that *independently* of the mechanism of neutrinoless double decay, the occurence of the latter implies a non-

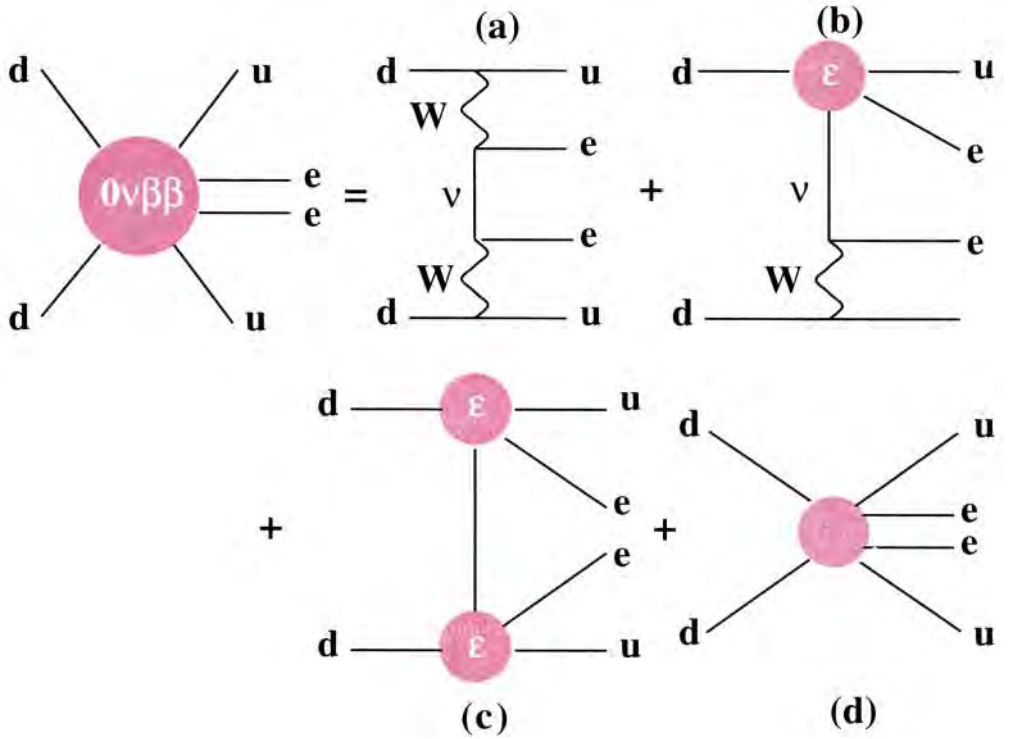

Fig. 1 Feynman graphs of the general double beta decay with long range (a-c) and short range (d) parts (see ref.[18]).

zero neutrino mass and vice versa [22]. This theorem has been extended to supersymmetry. It has been shown[23] that if the neutrino has a finite Majorana mass, then the sneutrino necessarily has a (B-L) violating 'Majorana' mass, too, independent of the mechanism of mass generation. The experimental signature of the neutrinoless mode is a peak at the Q-value of the decay.

Restricting to the Majorana mass mechanism, a measured half-life allows to deduce information on the effective Majorana neutrino mass $\langle m \rangle$, which is a superposition of neutrino mass eigenstates [13, 14].

$$[T^{0\nu}_{1/2}(0^+_i \to 0^+_f)]^{-1} = C_{mm}\frac{\langle m\rangle^2}{m_e^2} + C_{\eta\eta}\langle\eta\rangle^2 + C_{\lambda\lambda}\langle\lambda\rangle^2 + C_{m\eta}\langle\eta\rangle\frac{\langle m\rangle}{m_e} + C_{m\lambda}\langle\lambda\rangle\frac{\langle m_\nu\rangle}{m_e} \cdot + C_{\eta\lambda}\langle\eta\rangle\langle\lambda\rangle, \quad \ldots(4)$$

$$\langle m\rangle = |m^{(1)}_{ee}| + e^{i\phi_2}|m^{(2)}_{ee}| + e^{i\phi_3}|m^{(3)}_{ee}|\,, \quad \ldots(5)$$

where $m^{(i)}_{ee} \equiv |m^{(i)}_{ee}|\exp(i\phi_i)$ $(i = 1,2,3)$ are the contributions to $\langle m\rangle$ from individual mass eigenstates, with ϕ_i denoting relative Majorana phases connected with CP violation, and $C_{mm}, C_{\eta\eta}, \ldots$ denote nuclear matrix elements squared, which can be calculated (see, e.g., ref.[24]); for a review and some recent discussions see e.g., refs.[7,14-15,21,25-28]. Ignoring contributions from right-handed weak currents on the right-hand side of eq.1, only the first term remains.

The effective mass is closely related to the parameters of neutrino oscillation experiments, as can be seen from the following expressions

$$|m^{(1)}_{ee}| = |U_{e1}|^2 m_1, \quad \ldots(6)$$

$$|m^{(2)}_{ee}| = |U_{e2}|^2\sqrt{\Delta m^2_{21} + m_1^2}, \quad \ldots(7)$$

$$|m^{(3)}_{ee}| = |U_{e3}|^2\sqrt{\Delta m^2_{32} + \Delta m^2_{21} + m_1^2}. \quad \ldots(8)$$

Here, U_{ei} are entries of the neutrino mixing matrix, and $\Delta m^2_{ij} = |m_i^2 - m_j^2|$, with m_i denoting neutrino mass eigenstates. U_{ei} and Δm^2 can be determined from neutrino oscillation experiments.

The importance of $\langle m\rangle$ for solving the problem of the structure of the neutrino mixing matrix and in particular to fix the absolute scale of the neutrino mass spectrum which cannot be fixed by ν - oscillation experiments alone, has been discussed in detail in e.g. refs.[5-6].

Double beta experiments to date gave only *upper limits* for the effective mass. The most sensitive

limits[29-31] were *already* of striking importance for neutrino physics, excluding for example, in hot dark matter models, the small mixing angle (SMA) MSW solution of the solar neutrino problem[7,19,31,38-41] in degenerate neutrino mass scenarios.

The HEIDELBERG-MOSCOW double beta decay experiment in the Gran Sasso Underground Laboratory[7,19,31,38-41] searches for double beta decay of $^{76}Ge \longrightarrow ^{76}Se + 2e^- + (2\bar{\nu})$ since 1990. It is the most sensitive double beta experiment since nine years now. The experiment operates five enriched (to 86%) high-purity ^{76}Ge detectors, with a total mass of 11.5 kg, the active mass of 10.96 kg being equivalent to a source strength of 125.5 mol ^{76}Ge nuclei.

We have performed recently[43-45] a refined analysis of the data obtained during the period August 1990–May 2000[31]. This analysis concentrates on the neutrinoless decay mode which is the one relevant for particle physics (see, e.g. ref.[7]), and reports first evidence for the neutrinoless decay mode (see also refs.[46-50]). First reactions have been published in refs.[5,51-73]. For the results concerning $2\nu\beta\beta$ decay and Majoron-accompanied decay we refer to refs.[31,74] We shall describe here the results leading to the evidence for $0\nu\beta\beta$ decay. The results will then be put into the context of other present $\beta\beta$ activities.

2 Experimental Set-up and Results

A detailed description of the HEIDELBERG-MOSCOW experiment has been given recently in refs.[31,39]. Therefore only some important features will be given here. We start with some general notes.

1. Since the sensitivity for the $0\nu\beta\beta$ half-life is

$$T_{1/2}^{0\nu} \sim a \times \varepsilon \sqrt{\frac{Mt}{\Delta E B}} \qquad \ldots(9)$$

(and $\frac{1}{\sqrt{T^{0\nu}}} \sim \langle m_\nu \rangle$), with a denoting the degree of enrichment, ε the efficiency of the detector for detection of a double beta event, M the detector (source) mass, ΔE the energy resolution, B the background and t the measuring time, the sensitivity of our 11 kg *of enriched* ^{76}Ge experiment corresponds to that of an at least 1.2 ton *natural* Ge experiment. After enrichment, energy resolution, background and source strength are the most important features of a $\beta\beta$ experiment.

2. The high energy resolution of the Ge detectors of 0.2% or better, assures that there is no background for a $0\nu\beta\beta$ line from the two-neutrino double beta decay in this experiment, in contrast to most other present experimental approaches, where limited energy resolution is a severe drawback.

3. The efficiency of Ge detectors for detection of $0\nu\beta\beta$ decay events is close to 100 % (95%, see ref.[75].

4. The source strength in this experiment of 11 kg is the largest source strength ever operated in a double beta decay experiment.

5. The background reached in this experiment is, with 0.17 events/kg y keV in the $0\nu\beta\beta$ decay region (around 2000-2080 keV), the lowest limit ever obtained in such type of experiment.

6. The statistics collected in this experiment during 10 years of stable running is the largest ever collected in a double beta decay experiment.

7. The Q value for neutrinoless double beta decay has been determined recently with very high precision to be $Q_{\beta\beta}$=2039.006(50) keV[76,77].

We give now some experimental details. All detectors (whose technical parameters are given in Table I (see ref.[39])), except detector No. 4, are operated in a common Pb shielding of 30 cm, which consists of an inner shielding of 10 cm radiopure LC2-grade Pb followed by 20 cm of Boliden Pb. The whole setup is placed in an air-tight steel box and flushed with radiopure nitrogen in order to suppress the ^{222}Rn contamination of the air. The steel box is centered inside a 10-cm boron-loaded polyethylene shielding to decrease the neutron flux from outside. An active anticoincidence shielding is placed on top of the setup to reduce the effect of muons. Detector No. 4 is installed in a separate setup, which has an inner shielding of 27.5 cm electrolytical Cu, 20 cm lead, and boron-loaded polyethylene shielding below the steel box, but no muon shielding. Fig.2 gives a view of the experimental setup.

To check the stability of the experiment, a calibration with a ^{228}Th and a ^{152}Eu+^{228}Th, and a ^{60}Co source is done weekly. High voltage of the detectors, temperature in the detector cave and the computer room, the nitrogen flow in the detector boxes, the muon anticoincidence signal, leakage current of the detectors, overall and individual trigger rates are monitored daily. The energy spectrum is taken in 8192 channels in the range from threshold up to about 3 MeV, and in a parallel spectrum up to about 8 MeV.

Because of the big peak-to-Compton ratio of the large detectors, external γ activities are relatively eas-

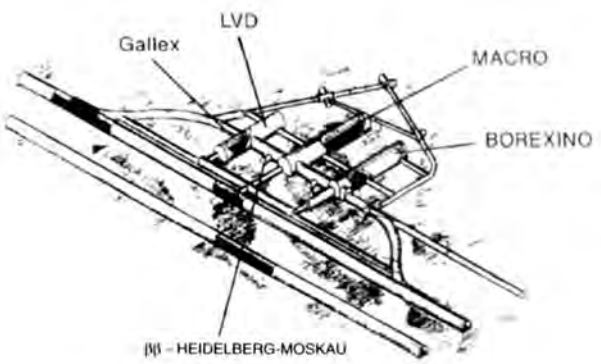

Fig. 2 The $\beta\beta$-laboratory of the HEIDELBERG-MOSCOW experiment in the Gran Sasso and its location between halls A and B, and four of the enriched detectors during installation (from top to bottom).

Table I

Technical parameters of the five enriched detectors. (FWHM - full width at half maximum.)

Detector Number	Total Mass [kg]	Active Mass [kg]	Enrichment in ^{76}Ge [%]	FWHM 1996 at 1332 keV [keV]	FWHM 2000 at 1332 keV [keV]
No. 1	0.980	0.920	85.9 ± 1.3	2.22 ± 0.02	2.42 ± 0.22
No. 2	2.906	2.758	86.6 ± 2.5	2.43 ± 0.03	3.10 ± 0.14
No. 3	2.446	2.324	88.3 ± 2.6	2.71 ± 0.03	2.51 ± 0.16
No. 4	2.400	2.295	86.3 ± 1.3	2.14 ± 0.04	3.49 ± 0.24
No. 5	2.781	2.666	85.6 ± 1.3	2.55 ± 0.05	2.45 ± 0.11

ily identified, since their Compton continuum is to a large extent shifted into the peaks. The background identified by the measured γ lines in the background spectrum consists of:

1. primordial activities of the natural decay chains from ^{238}U, ^{232}Th, and ^{40}K
2. anthropogenic radio nuclides, like ^{137}Cs, ^{134}Cs, ^{125}Sb, ^{207}Bi
3. cosmogenic isotopes, produced by activation due to cosmic rays. The activity of these sources in the setup is measured directly and can be located due to the measured and simulated relative peak intensities of these nuclei. Hidden in the continuous background are the contributions of
4. the bremsstrahlungs spectrum of ^{210}Bi (daughter of ^{210}Pb),
5. elastic and inelastic neutron scattering, and
6. direct muon-induced events.

External α and β activities are shielded by the 0.7-mm inactive zone of the p-type Ge detectors on the outer layer of the crystal. The enormous radiopurity of HP-germanium is proven by the fact that the detectors No. 1, No. 2 and No. 3 show no indication of any α peaks in the measured data. Therefore no contribution of the natural decay chains can be located inside the crystals. Detectors No. 4 and No. 5 seem to be slightly contaminated with ^{210}Pb on the level of few μBq/kg, most likely surface contaminations at the inner contact. This contamination was identified by a measured α peak in the background spectrum at 5.305 MeV of the daughter ^{210}Po and the constant time development of the peak counting rate. There is no contribution to the background in the interesting evaluation areas of the experiment due to this activity. For further details about the experiment and background we refer to refs.[39,75] (see also Table II).

In the vicinity of the Q-value of the double beta decay of $Q_{\beta\beta}$ = 2039.006(50) keV, very weak lines at 2034.744 and 2042 keV from the cosmogenic nuclide ^{56}Co, and from ^{214}Bi (^{238}U-decay chain) at 2010.7, 2016.7, 2021.8 and 2052.9 keV, may be expected.

On the other hand, there are no background γ-lines at the position of an expected $0\nu\beta\beta$ line, according to our Monte Carlo analysis of radioactive impurities in the experimental setup[75] and according to the compilations in ref.[78].

In total 55 possible γ-lines from various isotopes in the region between 2037 and 2041 keV are known [78]. Only 5 of the isotopes responsible for them (^{102}Rh, ^{146}Eu, ^{124}I, ^{124}Sb and ^{170}Lu) have half-lifes larger than 1 day. However, some of the isotopes yielding lines in this energy range can in principle be produced by inelastic hadron reactions (induced by muons or neutrons).

Therefore each of these 55 isotopes was checked for the existence of a γ-line from the isotope which has a high emission probability I_h. A search was made for this γ-line in the *measured* spectrum to obtain its intensity (S_h) or an upper limit for it. Then the adopted intensity S_0 for a γ-line from the same isotope in the area around ~2039 keV can be calculated by using the emission probability I_0 for the line at ~2039 keV. Different absorption for gammas of different energies are taken into account in a schematic way.

If the calculated intensity $S_l < 1$ for the γ-line in the

Table II

*Development of the experimental set-up and of the background numbers in the different data acquisition periods for the enriched detectors of the HEIDELBERG-MOSCOW experiment. *) Without PSA method.*

Detector Number	Life Time [days]	Date Start	End	Shielding Cu	Pb	boron-poly.	Background*) [counts/ keV y kg] 2000.-2100. keV	PSA
No.1	387.6	8/90	8/91	yes			0.56	no
		1/92	8/92					no
No.2	225.4	9/91	8/92		yes		0.29	no
Common shielding for three detectors								
No.1	382.8	9/92	1/94		yes		0.22	no
No.2	383.8	9/92	1/94		yes		0.22	no
No.3	382.8	9/92	1/94		yes		0.21	no
No.1	263.0	2/94	11/94		yes	yes	0.20	no
No.2	257.2	2/94	11/94		yes	yes	0.14	no
No.3	263.0	2/94	11/94		yes	yes	0.18	no
Full Setup **Four detectors in common shielding, one detector separate**								
No.1	203.6	12/94	8/95		yes	yes	0.14	no
No.2	203.6	12/94	8/95		yes	yes	0.17	no
No.3	188.9	12/94	8/95		yes	yes	0.20	no
No.5	48.0	12/94	8/95		yes	yes	0.23	since 2/95
No.4	147.6	1/95	8/95	yes			0.43	no
No.1	203.6	11/95	05/00		yes	yes	0.170	no
No.2	203.6	11/95	05/00		yes	yes	0.122	yes
No.3	188.9	11/95	05/00		yes	yes	0.152	yes
No.5	48.0	11/95	05/00		yes	yes	0.159	yes
No.4	147.6	11/95	05/00	yes			0.188	yes

Table III

Possible reactions (second line) which could produce the isotopes listed in the first line (see ref.[18]).

isotope	^{52m}Fe	^{93m}Ru	^{120}In	^{170m}Ho	^{198}Tl
production reaction	^{50}Cr$(\alpha,2n\gamma)$	^{92}Mo$(\alpha,3n)$	^{120}Sn(n,p), ^{123}Sb(n,α)	^{170}Er(n,p)	^{197}Au$(\alpha,3n\gamma)$

interesting area, this isotope can be safely excluded to contribute a significant part to the background.

For example, the isotope ^{139}Xe possesses a γ-line at 2039.1 keV with an emission probability of 0.078%. This isotope also possesses a γ-line at 225.4 keV with an emission probability of 3.2%. The intensity of the line at 225.4 keV in our spectrum was measured to be <6.5 counts. This means that the γ-line at 2039.1 keV has $< 2\frac{0.078}{3.2}6.5 = 0.32$ counts, and therefore can be excluded.

Only eight isotopes could contribute a few counts according to the calculated limits, in the interesting area for the $0\nu\beta\beta$ -decay area: ^{52m}Fe, ^{93m}Ru, ^{120}In, ^{131}Ce, ^{170}Lu, ^{170m}Ho, ^{174}Ta and ^{198}Tl. Most of them have a half-life of a few seconds, only ^{170}Lu has a half-life of 2.01 days, and none of them has a longer living mother isotope. To contribute to the background they must be produced with a constant rate, e.g. by inelastic neutron and/or muon reactions. Only 5 isotopes can be produced in a reasonable way, by the reactions listed in Table III.

Except ^{120}Sb each of the target nuclides is stable. All reactions induced with α-particles can be excluded due to the very short interaction length of α-particles. Two possibilities remaining to explain possible events in the $0\nu\beta\beta$ -decay area would be:

- ^{120}Sn$(n,p)^{120}$In:
  The cross section for this reaction[81] is 2.5±1 mb for $E_n = 14.5$ MeV. Assuming a neutron flux of $(0.4\pm0.4)\times10^{-9}/cm^2/s$ for neutrons with an energy between 10-15 MeV as measured in the Gran Sasso[82] the rate of ^{120}In atoms produced per year is about 2×10^{-5} when there are 50 g of ^{120}Sn in the detector setup. Even when the cross-section is larger for lower energies, this cannot contribute a significant number of counts to the background.

- ^{170}Er$(n,p)^{170m}$Ho:
  The cross section for this reaction[83] is about 1.13 ±1 mb for $E_n = 14.8$ MeV. Assuming again a neutron flux of $(0.4\pm0.4)\times10^{-9}/cm^2/s$ for neutrons with an energy between 10-15 MeV the rate of ^{170}Er atoms produced per year is even less when assuming 50 g of ^{120}Er in the detector-setup.

In both cases it would not be understandable, how such large amounts of ^{120}Sn or ^{170}Er could have come into the experimental setup. Concluding we do not find indications for any nuclides, that might produce γ-lines with an energy around 2039 keV in the experimental setup.

Fig.3 shows the combined spectrum of the five enriched detectors obtained over the period August 1990 - May 2000, with a statistical significance of 54.981 kg y (723.44 molyears). (Note that in Fig. 1 of ref.[31]) only the spectrum of the first detector is shown, but normalized [87] to 47.4 kg y). The identified background lines give an indication of the stability of the electronics over a decade of measurements. The average rate (sum of all detectors) observed over the measuring time, has proven to be constant within statistical variations.

Fig.4 shows the part of the spectrum shown in Fig.3, in more detail around the Q-value of double beta decay. Fig.5 shows the spectrum of single site events (SSE) obtained for detectors 2,3,5 in the period November 1995 - May 2000, under the restriction that the signal simultaneously fulfills the criteria of *all three* methods of pulse shape analysis we have recently developed[84,86] and with which we operate all detectors except detector 1 (significance 28.053 kg y) since 1995.

Double beta events are single site events confined to a few mm region in the detector corresponding to the track length of the emitted electrons In all three method, mentioned above. the output of the charge-sensitive preamplifiers was differentiated with 10-20 ns sampled with 250 MHz and analysed off-line. The methods differ in the analysis of the measured pulse shapes. The first one relies on the broadness of the charge pulse maximum, the second and third one are based on neural networks. All three methods are 'calibrated' with known double escape (mainly SSE) and total absorption (mainly MSE) γ-lines[75,84–86]. They allow to achieve about 80% detection efficiency for both interaction types.

The expectation for a $0\nu\beta\beta$ signal would be a line of single site events on some background of multiple site events but also single site events. the latter coming to a large extent from the continuum of the 2614 keV γ-line from ^{208}Tl (see, e.g., the simulation in[84]). From simulation we expect that about 5% of the double beta single site events should be seen as MSE. This is caused by bremsstrahlung of the emitted electrons[75].

Installation of PSA has been performed in 1995 for

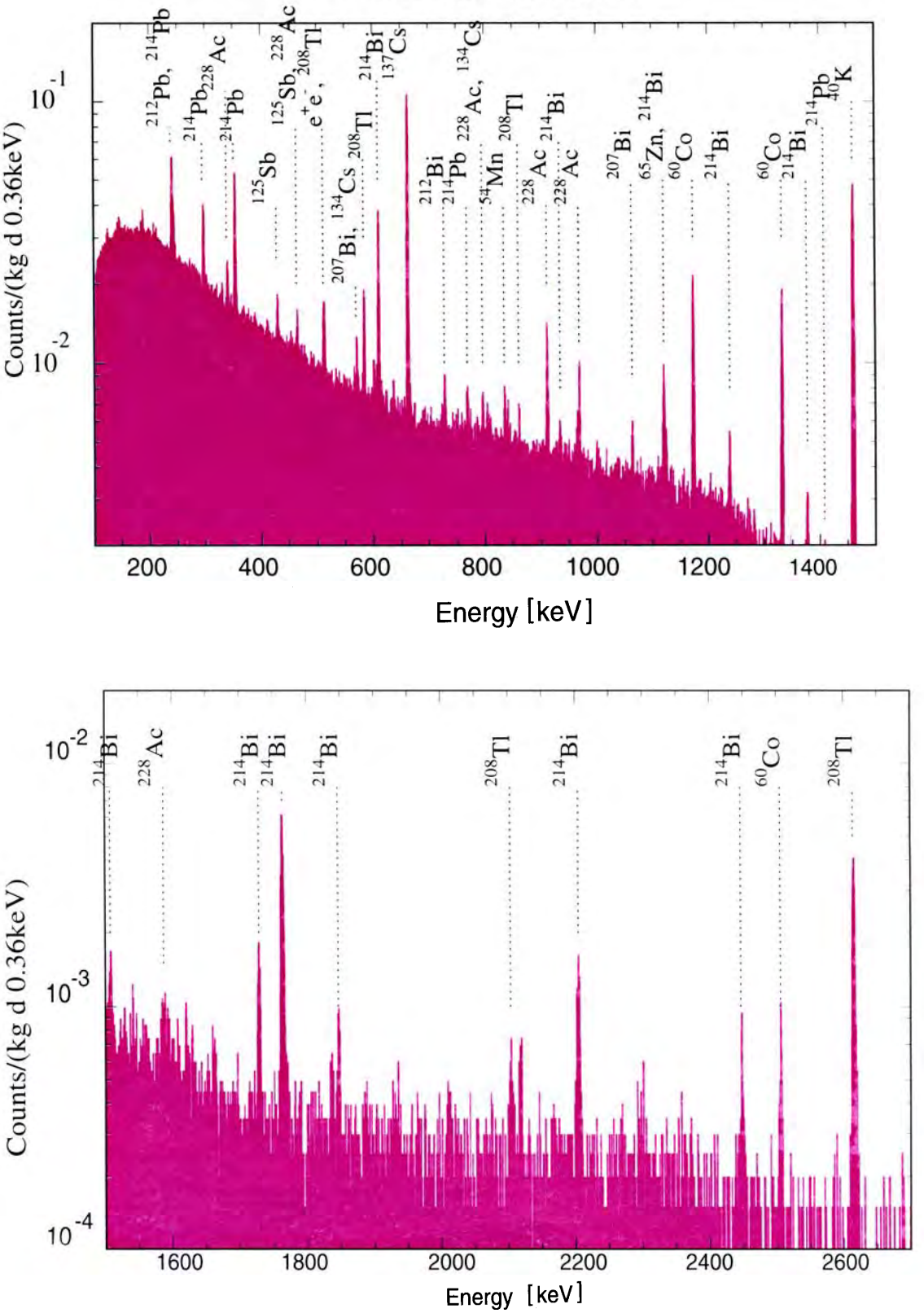

Fig. 3 Sum spectrum of enriched detectors Nr. 1,2,3,4,5 over the period August 1990 - May 2000 (54.9813 kg y) measured in the HEIDELBERG-MOSCOW experiment (binning 0.36 keV). The sources of the main identified background lines are noted.

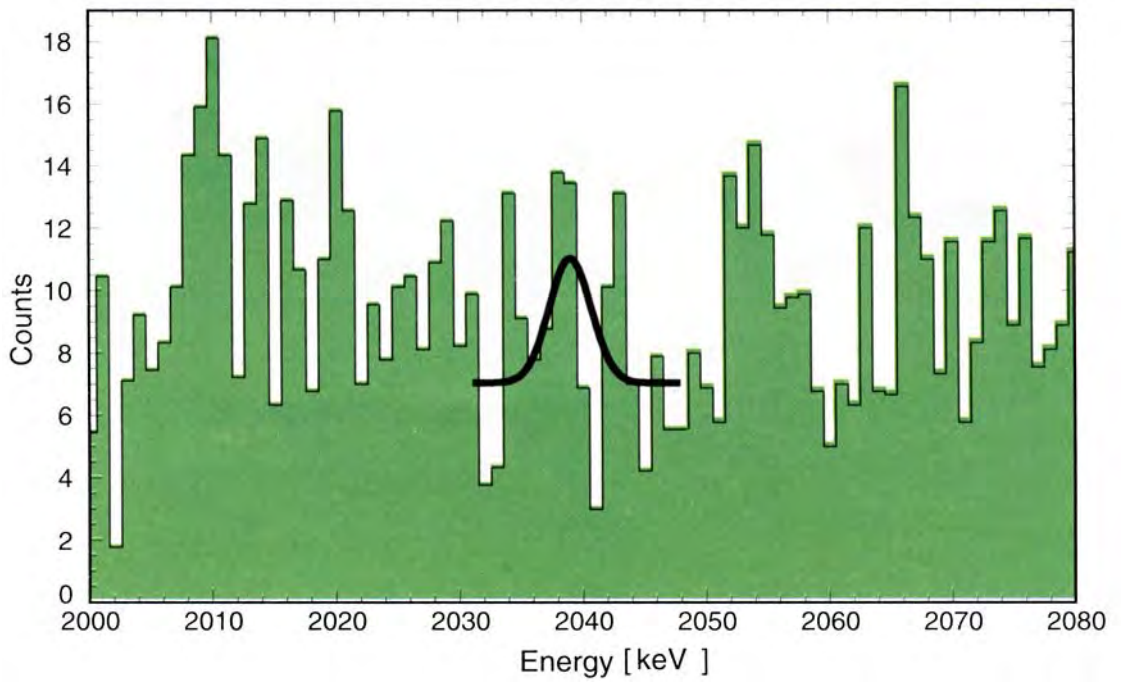

Fig. 4 Sum spectrum of the ^{76}Ge detectors Nr. 1,2,3,4,5 over the period August 1990 to May 2000, (54.9813 kg y) in the energy interval 2000 - 2080 keV, around the $Q_{\beta\beta}$ value of double beta decay ($Q_{\beta\beta}$ = 2039.006(50) keV) summed to 1 keV bins. The curve results from Bayesian inference in the way explained in sec.3. It corresponds to a half-life $T^{0\nu}_{1/2}$=(0.80 - 35.07)× 10^{25} y (95% c.l.)

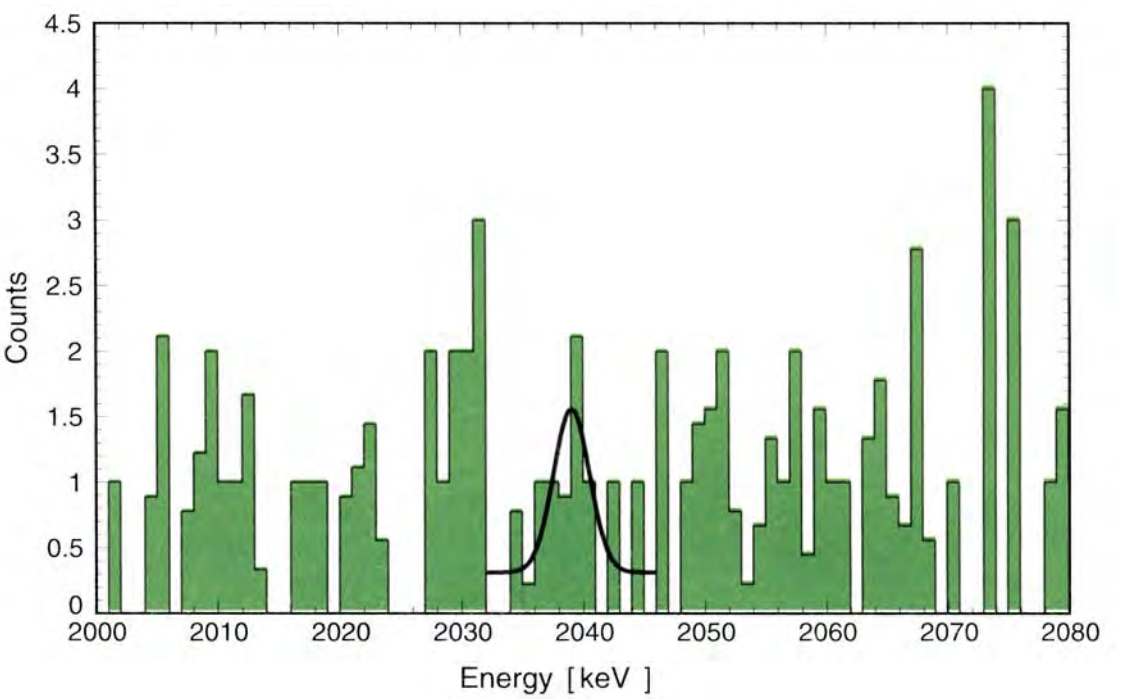

Fig. 5 Sum spectrum of single site events, measured with the detectors Nr. 2,3,5 operated with pulse shape analysis in the period November 1995 to May 2000 (28.053 kg y), summed to 1 keV bins. Only events identified as single site events (SSE) by all three pulse shape analysis methods[84–86] have been accepted. The curve results from Bayesian inference in the way explained in sec.3. When corrected for the efficiency of SSE identification (see text), this leads to the following value for the half-life: $T^{0\nu}_{1/2}$=(0.88 - 22.38)× 10^{25} y (90% c.l.).

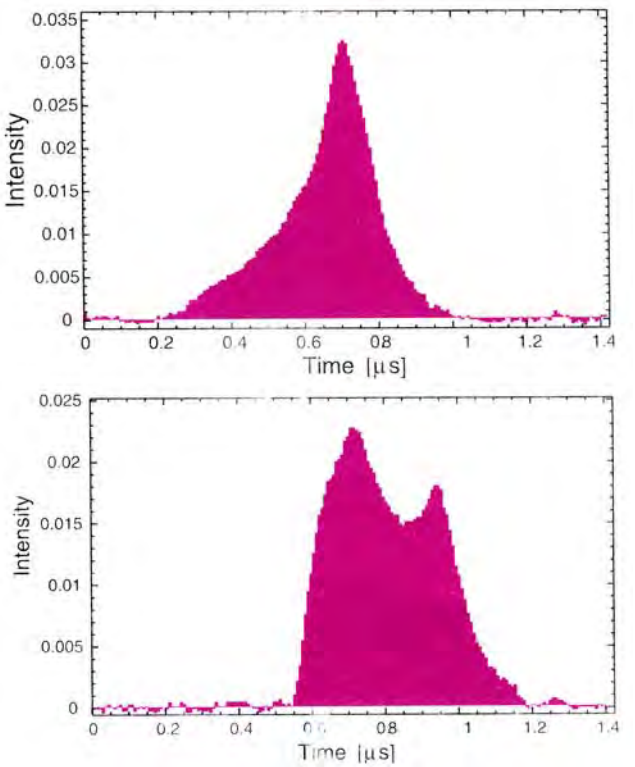

Fig. 6 Top: Shape of one candidate for $0\nu\beta\beta$ decay classified as SSE by all three methods of pulse shape discrimination. Bottom: Shape of one candidate classified as MSE by all three methods.

the four large detectors. Detector 5 runs since February 1995, detectors 2,3,4 since November 1995 with PSA. The measuring time with PSA from November 1995 until May 2000 is 36.532 kg years, for detectors 2,3,5 it is 28.053 kg y. Fig.6 shows typical SSE and MSE events from our spectrum.

All the spectra are obtained after rejecting coincidence events between different Ge detectors and events coincident with activation of the muon shield. The spectra, which are taken in bins of 0.36 keV, are shown in Figs. 4, 5 & (Fig.2 of ref.[43]) in 1 keV bins, which explains the broken number in the ordinate. We do the analysis of the measured spectra with (Fig. 4) and without the data of detector 4 (see Fig.2 in ref.[43], 46.502 kg y) since the latter does not have a muon shield and has the weakest energy resolution. The 0.36 keV bin spectra are used in all analyses described in this work. We ignore for each detector the first 200 days of operation, corresponding to about three half-lives of ^{56}Co ($T_{1/2}$ = 77.27 days), to allow for some decay of short-lived radioactive impurities.

Table IV

Energies and widths of some prominent lines in the sum spectrum of all five detectors determined by our energy calibration and peak fit methods, and comparison with the energy given in the literature[78], and the fitted dependence of the width as function of energy.

energy [keV] fit	energy [keV] from [78]	width [keV] fit	width [keV] from calc.
1460.81 ± 0.02	1460.81	1.49 ± 0.01	1.49 ± 0.13
1764.56 ± 0.05	1764.49	1.70 ± 0.05	1.59 ± 0.15
2103.31 ± 0.45	2103.53	1.86 ± 0.35	1.71 ± 0.16
2204.12 ± 0.14	2204.19	1.89 ± 0.13	1.74 ± 0.17
2447.73 ± 0.26	2447.86	1.82 ± 0.33	1.82 ± 0.18
2614.48 ± 0.07	2614.53	1.80 ± 0.06	1.88 ± 0.18

The background rate in the energy range 2000 - 2080 keV is found to be (0.17 ± 0.01) events/ kg y keV (*without* pulse shape analysis) considering *all* data as background. This is the lowest value ever obtained in such type of experiments. The energy resolution at the $Q_{\beta\beta}$ value in the sum spectra is extrapolated from the strong lines in the spectrum to be (4.00 ± 0.39) keV in the spectra with detector 4, and (3.74 ± 0.42) keV (FWHM) in the spectra without detector 4 (see Fig.7 & Table IV. The energy calibration of the experiment has an uncertainty of 0.20 keV (Table IV & Fig.8).

3 Data Analysis

We analysed the measured spectra with the following methods:

1. *Bayesian method*, which is used widely at present in nuclear and astrophysics (see, e.g. refs.[88-91]). This method is particularly suited for low counting rates, where the data follow a Poisson distribution, that cannot be approximated by a Gaussian. It has been used also in on earlier double beta experiment already[92]
2. *Feldman-Cousins Method*[93, 89]
3. *Maximum Likelihood Method (see ref.[89,94]).*

The application of the Bayesian method in our experiment is described in refs.[44-45]. Some numerical examples of the sensitivities of Bayesian and of the Maximum Likelihood Methods in the search for events of low statistics are given in the next section and in refs.[44-45,48-49].

Numerical Simulations

To check the methods of analysing the measured data (Bayes and Maximum Likelihood Method), and in particular to check the programs we wrote, we have generated spectra and lines with a random number

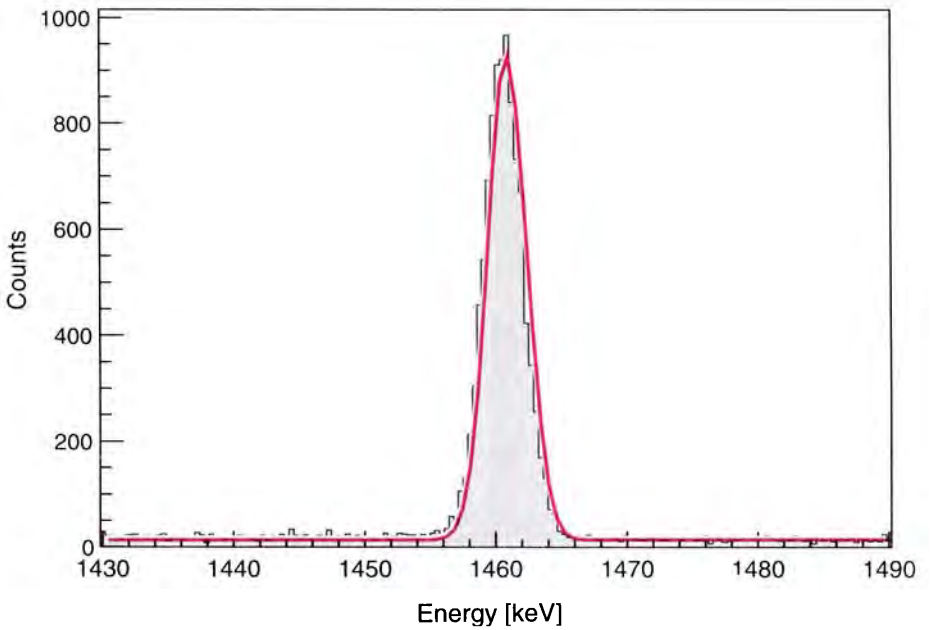

Fig. 7 Fit of one the lines (here the 1460.81 keV line from ^{40}K) in the sum spectrum of all five detectors, used for the calibration and the determination of the energy resolution (see Table IV).

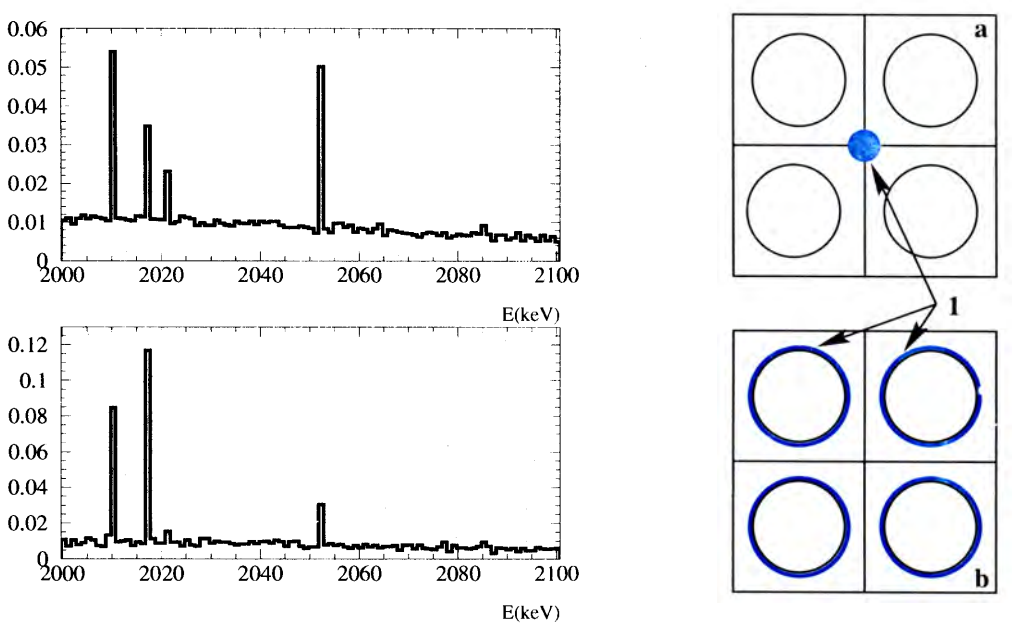

Fig. 8 Demonstration of the dependence of the relative intensities of the weak ^{214}Bi lines on the location of the impurity in the experimental setup. The right side shows two different locations of the impurity (1) relative to the detectors. The left side shows the corresponding different relative intensities to be expected. Top: Source in some distance from the detectors (as in a) (right part). Bottom: Source in copper cap very near around the detectors (as in b) (right part). The ordinate shows relative intensities (see ref.[44]).

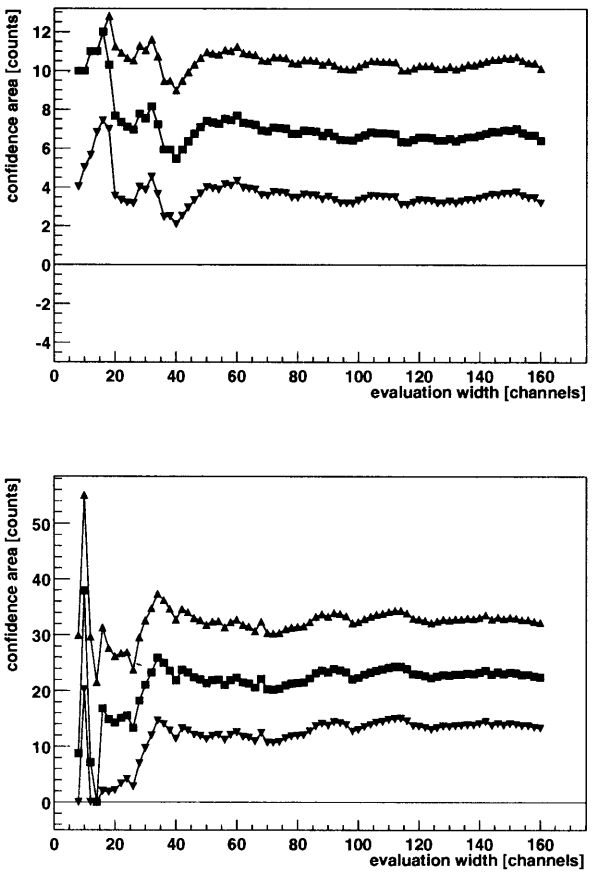

Fig. 9 Top: Analysis of simulated spectrum with Gaussian peak of 5 events and FWHM of 9.4 channels on a Poisson-distributed background spectrum of 0.5 events/channel, as function of interval of analysis. The middle line is the best value. Upper and lower lines correspond to the 68.3% confidence limits. Bottom: The same as above, but the peak contains 20 events, the background is 4 events/channel. One channel corresponds to 0.36 keV in our measured spectra.

generator and performed then a Bayes and Maximum Likelihood analysis (see refs.[44-45]). The length of each generated spectrum is 8200 channels, with a line located at bin 5666, the width of the line (sigma) being 4 channels (These special values have been chosen so that every spectrum is analogue to the measured data). The creation of a simulated spectrum is executed in two steps, first the background and second the line was created, using random number generators available at CERN (see ref.[95]). In the first step, a Poisson random number generator was used to calculate a random number of counts for each channel, using a mean value of μ=4 or $\mu = 0.5$, respectively, in the Poisson distribution

$$P(n) = \frac{\mu^n}{n!} e^{-\mu} \qquad \ldots(10)$$

These mean values correspond roughly to our mean background measured in the spectra with or without pulse shape analysis.

In the second step, a Gaussian random number generator was used to calculate a random channel number for a Gaussian distribution with a mean value of 5666 (channel) and with a sigma of 4 (channels). The contents of this channel then is increased by one count. This Gaussian distribution filling procedure was repeated for n times, n being the number of counts in this line.

For each choice of μ and n, 100 different spectra were created, and analysed subsequently with two different methods: the maximum likelihood method (using the program set of ref.[94]) and the Bayes-method. Each method, when analysing a spectrum, gives a lower and an upper limit for the number of counts in the line for a given confidence level c (e.g. $c = 95\%$) (let us call it *confidence area A*). A confidence level of 95% means, that in 95% of all cases the true value should be included in the calculated confidence area. This should be exactly correct when analysing an infinite number of created spectra. When using 100 spectra, as done here, it should be expected that this number is about the same. Now these 100 spectra with a special n and μ are taken to calculate a number d, which is the number of that cases, where the true value n is included in the resulting confidence area A.

This number d is given in Table V for the results of the two different analysis methods and for various values for μ and n. It can be seen that the Bayes method reproduces even the smallest lines properly, while the Maximum Likehood method has some limitations there.

Another test has been performed. We generated 1000 simulated spectra containing *no* line. Then the probability has been calculated with the Bayesian method that the spectrum *does* contain a line at a given energy. Table VI presents the results: the first column contains the corresponding confidence limit c (precisely the parameter K_E defined earlier), the second column contains the *expected* number of spectra indicating existence of a line with a confidence limit above the value c and the third column contains the number

Table V

Results from the analysis of the simulated spectra using a mean background of 4 and 0.5 counts, and different line intensities. The number d of cases, where the true number of counts in the line (given in the left column), is found in the calculated confidence area is given in the second or third column for the Bayes method, and in the fourth and fifth column for the maximum likelihood method. For details see text.

	4 counts				0.5 counts			
counts	Bayes		Max. Lik.		Bayes		Max. Lik.	
in line	68%	95%	68%	95%	68%	95%	68%	95%
0	81	98	60	85	81	99	62	84
5	88	98	68	80	75	100	82	98
10	74	97	74	90	86	100	84	100
20	73	96	77	94	90	100	92	100
100	90	98	87	99	95	100	99	100
200	83	99	78	99	92	100	100	100

Table VI

Number of spectra with a calculated confidence limit above a given value. For details see text.

C.L.	Expected	Found
90.0%	100 ± 31	96
95.0%	50 ± 7	42
99.0%	10 ± 3	12
99.9%	1 ± 1	0

of spectra with a confidence limit above the value c, found in the simulations. The result underlines that K_E here is equivalent to the usual confidence level of classical statistics.

We further investigated with the computer generated spectra the dependence of the peak analysis on the width of the energy range of evaluation. Two examples are shown in Fig.9. Here the contents of the simulated peak found with the Bayes method is shown as function of the analysis interval given in channels (one channel corresponds to 0.36 keV in our measured spectra). The line in the middle is the best-fit value of the method, the upper and lower lines correspond to the upper and lower 68.3% confidence limits. In the upper figure the true number of counts in the simulated line was 5 events, on a Poisson-distributed background of 0.5 events/channel, in the lower figure it was 20 events on a background of 4 events/channel. It can be seen that the analysis gives safely the correct number of counts, when choosing an analysis interval of not less than 40 channels.

Analysis of the Full Data

We first concentrate on the full spectra (see Fig.4, and Fig.2 in ref.[43]), without *any* data manipulation (no background subtraction, no pulse shape analysis). For the evaluation, we consider the *raw data* of the detectors.

The Bayesian peak finding procedure described in refs.[43-45] determines the probability that a line with correct width, and Gaussian shape, exists at given energy E, assuming the rest of the spectra in the interval of analysis as (constant) background. It leads for the measured spectra to the result shown on the left hand sides of Figs.10,11. For every energy E in the spectral range 2000 -2080 keV, we have determined the probability K_E that there is a line at E. All the remainder of the spectrum was considered to be background in this search.

The peak detection procedure yields lines at the positions of known[78] weak γ-lines from the decay of ^{214}Bi at 2010.7, 2016.7, 2021.8 and 2052.9 keV. The lines at 2010.7 and 2052.9 keV are observed at a confidence level of 3.7 and 2.6σ, respectively. The observed intensities are consistent with the expectations from the strong Bi lines in our spectrum, and the branching ratios given in ref.[78], within about the 2σ experimental error (see Table VII and ref.[74]). The expectations here are calculated including summing effects of consecutive γ-lines (so-called True Coincidence Summing - TCS), by Monte-Carlo simulation of our set-up. *Only* in this way the strong dependence of the relative intensities on the location of the impurities in the set-up can be properly taken into account (see Fig.8).

In addition, a line centered at 2039 keV shows up. This is compatible with the Q-value[76,77] of the double beta decay process. We emphasize, that at this energy no γ-line is expected according to the compilations in ref.[78] (see discussion in section 2). Figs.10,11 do not show indications for the lines from ^{56}Co at 2034.7 keV and 2042 keV discussed earlier[75]. In addition to the line at 2039 keV we find candidates for lines at energies beyond 2060 keV and around 2030 keV, which at present cannot be attributed. This is a task of nuclear spectroscopy.

It is of interest that essentially the same lines as

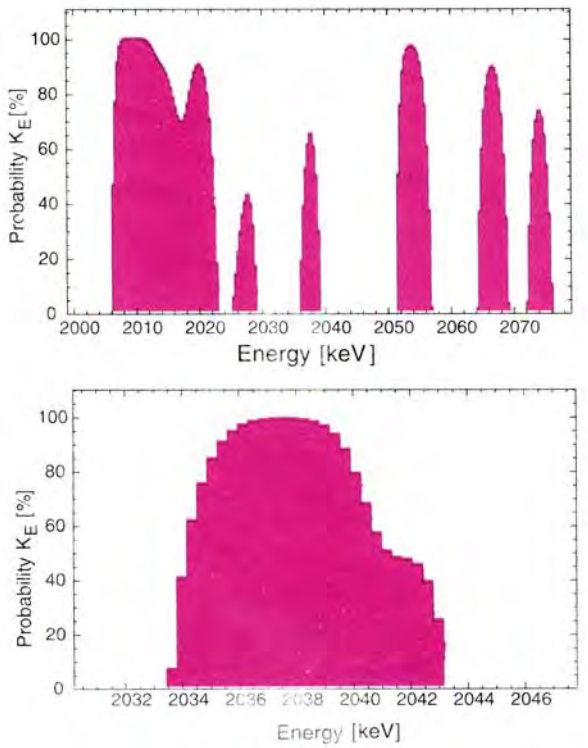

Fig. 10 Scan for lines in the full spectrum taken from 1990-2000 with detectors Nr. 1,2,3,4,5, (Fig.4), with the Bayesian method of sec. 3.1. The ordinate is the probability K_E that a line exists as defined in the text. Top: Energy range 2000 - 2080 keV. Bottom: Energy range of analysis $\pm 5\sigma$ around $Q_{\beta\beta}$.

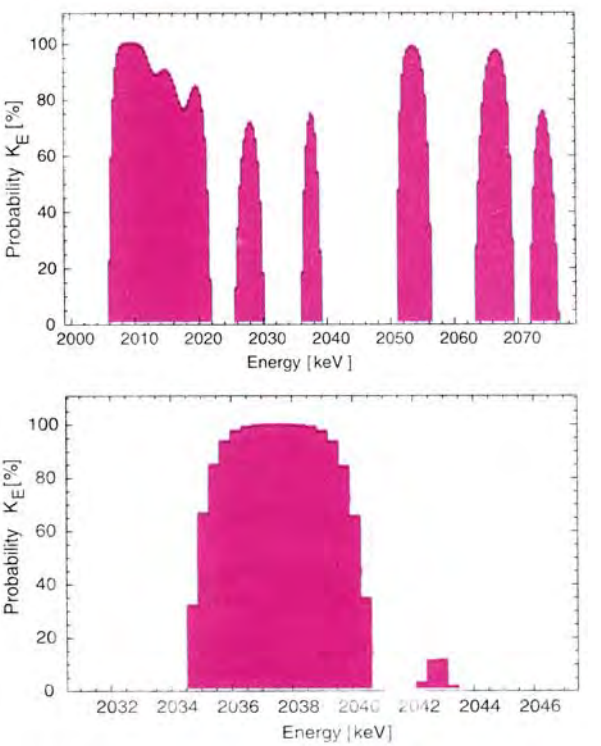

Fig. 11 Top: Probability K_E that a line exists at a given energy in the range of 2000-2080 keV derived via Bayesian inference from the spectrum taken with detectors Nr. 1,2,3,5 over the period August 1990 to May 2000, 46.502 kg y (see Fig.2 from ref.[43].) Bottom: Result of a Bayesian scan for lines as in the left part of this figure, but in the energy range of analysis $\pm 5\sigma$ around $Q_{\beta\beta}$.

found by the peak scan procedure in Figs.10,11,12, are found[45, 74] when doing the same kind of analysis with the best existing *natural* Ge experiment of D. Caldwell et al.[92], which has a by a factor of ~4 better statistics *of the background*. This experiment does however, see the line at 2039 keV (see section 3.5).

Bayesian peak detection (the same is true for Maximum Likelihood peak detection) of our data suggests a line at $Q_{\beta\beta}$ whether or not one includes detector Nr. 4 without muon shield (Figs.10,11). The line is also suggested in Fig.12 after removal of multiple site events (MSE), see below.

On the top panels of Figs. 10,11,12, the background intensity identified by the Bayesian procedure is too high because the procedure averages the background over all the spectrum (*including* lines) *except* for the line it is trying to single out. Inclusion of the known lines into the fit naturally improves the background. As example, we show in Fig. 13 the spectrum of Fig. 4 (here in the original 0.36 keV binning) with a simultaneous fit of the range 2000 - 2100 keV (assuming lines at 2010.78, 2016.70, 2021.60, 2052.94, 2039.0 keV and two lines at higher energy). The probability for a line in this fit at 2039 keV is 91%. Finally, on the right-hand side of Figs.10,11 (and also Fig. 12) the peak detection procedure is carried out within an energy interval that seems to not contain (according to the top panel) lines other than the one at $Q_{\beta\beta}$. This interval is broad enough (about $\pm$ 5 standard deviations of the Gaussian line, i.e. as typically used in search for resonances in high-energy physics) for a meaningful analysis (see Fig.9 in section 3.2). We find, with the Bayesian method, the probability $K_E = 96.5\%$ that there is a line at 2039.0 keV in the spectrum shown in Fig.4. This is a confidence level of 2.1 σ in the usual language. The number of events is found to be 0.8 to 32.9 (7.6 to 25.2) with 95% (68%) c.l., with

Table VII

^{214}Bi is product of the ^{238}U natural decay chain through β^- decay of ^{214}Pb and α decay of ^{218}At. It decays to ^{214}Po by β decay. Shown in this Table are the measured intensities of ^{214}Bi lines in the spectrum shown in Fig.1 of ref.[43] in the energy window 2000 - 2060 keV, our calculation of the intensities expected on the basis of the branching ratios given in Table of Isotopes[78], with and without simulation of the experimental setup, and the intensities expected by Aalseth et al. hep-ex/0202018, who do not simulate the setup and thus ignore summing of the γ energies (see ref.[79]).

Energy* (keV)	Intensity of Heidelberg-Mos.Exper.	σ	Branching Ratios[78] [%]	Simul. of Experim. Setup+	Expect. rate acc. to sim.**)	Expect. rate++ acc. to ref.[78] ++)	Aalseth et al.*** (see ref.[79])
609.312(7)	4399±92		44.8(5)	5715270±2400			
1764.494(14)	1301±40		15.36(20)	1558717±1250			
2204.21(4)	319±22		4.86(9)	429673±656			
2010.71(15)	37.8±10.2	3.71	0.05(6)	15664±160	12.2±0.6	4.1±0.7	0.64
2016.7(3)	13.0±8.5	1.53	0.0058(10)	20027±170	15.6±0.7	0.5±0.1	0.08
2021.8(3)	16.7±8.8	1.90	0.020(6)	1606±101	1.2±0.1	1.6±0.5	0.25
2052.94(15)	23.2±9.0	2.57	0.078(11)	5981±115	4.7±0.3	6.4±1	0.99
2039.006	12.1±8.3	1.46					

**) We have considered for comparison the 3 strongest ^{214}Bi lines, leaving out the line at 1120.287 keV (in the measured spectrum this line is partially overimposed on the 1115.55 keV line of ^{65}Zn). The number of counts in each line have been calculated by a maximum-likelihood fit of the line with a gaussian curve plus a constant background.*

+) The simulation is performed assuming that the impurity is located in the copper part of the detector chamber (best agreement with the intensities of the strongest lines in the spectrum). The error of a possible misplacement is not included in the calculation. The number of simulated events is 10^8 for each of our five detectors.

***) This result is obtained normalizing the simulated spectrum to the experimental one using the 3 strong lines listed in column one. Comparison to the neighboring column on the right shows that the expected rates for the weak lines can change strongly if we take into account the simulation. The reason is that the line at 2010.7 keV can be produced by summing of the 1401.50 keV (1.55%) and 609.31 keV (44.8%) lines, the one at 2016.7 keV by summing of the 1407.98 (2.8%) and 609.31 (44.8%) lines; the other lines at 2021.8 keV and 2052.94 keV do suffer only very weakly from the summing effect because of the different decay schemes.*

++) This result is obtained using the number of counts for the three strong lines observed in the experimental spectrum and the branching ratios from [78], but without simulation. For each of the strong lines the expected number of counts for the weak lines is calculated and then an average of the 3 expectations is taken.

****) Without simulation of the experimental setup. The numbers given here are close to those in the neighboring left column, when taking into account that Aalseth et al. refer to a spectrum which has only ~11% of the statistics of the spectrum shown in Fig.1 of ref.[43].*

best value of 16.2 events. For the spectrum shown in Fig. 2 in ref.[43], we find a probability for a line at 2039.0 keV of 97.4% (2.2 σ). In this case the number of events is found to be 1.2 to 29.4 with 95% c.l.. It is 7.3 to 22.6 events with 68.3% c.l.. The most probable number of events (best value) is 14.8 events. These values are stable against small variations of the interval of analysis, as expected from Fig. 9 in section 3.2. For example, changing the lower and upper limits of the interval of analysis between 2030 and 2032 and 2046 and 2050 yields consistently values of K_E between 95.3 and 98.5% (average 97.2%) for the spectrum of Fig.2 of ref.[43].

We also applied the Feldman-Cousins method recommended by the Particle Data Group[93, 89]. This method (which does not use the information that the line is Gaussian) finds a line at 2039 keV on a confidence level of 3.1 σ (99.8% c.l.).

Analysis of Single Site Events Data

From the analysis of the single site events (Fig.5), we find after 28.053 kg y of measurement 9 SSE events in the region 2034.1–2044.9 keV (± 3σ around $Q_{\beta\beta}$). (Fig.14). Analysis of the single site event spectrum (Fig.5), as described in section 3.1, shows again evidence for a line at the energy of $Q_{\beta\beta}$ (Fig.12). Analyzing the range of 2032 - 2046 keV, we find the probability of 96.8% that there is a line at 2039.0 keV. We thus see a signal of single site events, as expected for neutrinoless double beta decay, at the $Q_{\beta\beta}$ value obtained in the precision experiment of ref.[76]. The analysis of the line at 2039.0 keV before correction

for the efficiency yields 4.6 events (best value) or (0.3 - 8.0) events within 95% c.l. ((2.1 - 6.8) events within 68.3% c.l.). Corrected for the efficiency to identify an SSE signal by successive application of all three PSA methods, which is 0.55 ± 0.10, we obtain a $0\nu\beta\beta$ signal with 92.4% c.l.. The signal is (3.6 - 12.5) events with 68.3% c.l. (best value 8.3 events). Thus, with proper normalization concerning the running times (kg y) of the full and the SSE spectra, we see that almost the full signal remains after the single site cut (best value), while the ^{214}Bi lines (best values) are considerably reduced (see Fig.15).

We have used a ^{238}Th source to test the PSA method. We find the reduction of the 2103 keV and 2614 keV ^{228}Th lines (known to be multiple site or mainly multiple site), relative to the 1592 keV ^{228}Th line (known to be single site), shown in Fig.15. This proves that the PSA method works efficiently. Essentially the same reduction as for the Th lines at 2103 and 2614 keV and for the weak Bi lines is found for the strong ^{214}Bi lines (e.g. at 609.6 and 1763.9 keV (Fig.15)).

The Feldman-Cousins method gives a signal at 2039.0 keV of 2.8 σ (99.4%). The possibility, that the single site signal at 2039.0 keV is the double escape line corresponding to a (much more intense!) full energy peak of a γ-line at 2039+1022=3061 keV is excluded from the high-energy part of our spectrum.

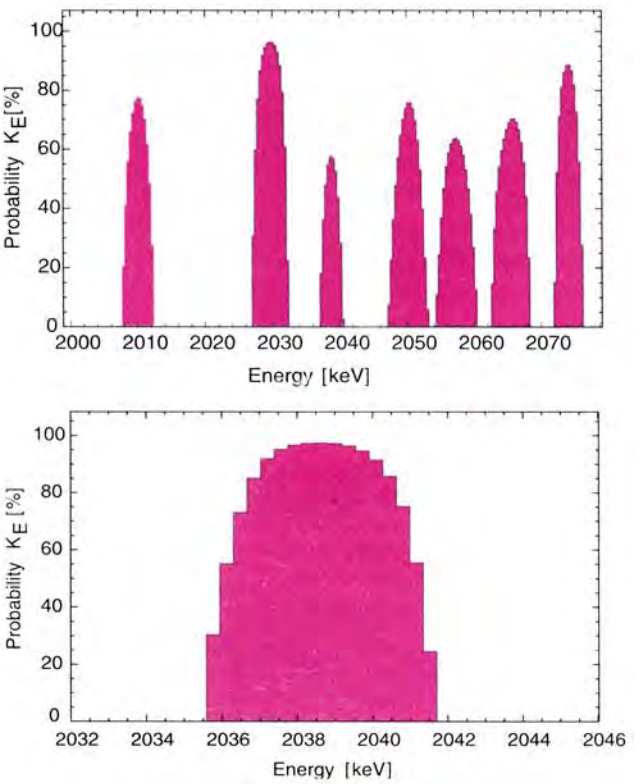

Fig. 12 Scan for lines in the single site event spectrum taken from 1995-2000 with detectors Nr. 2,3,5, (Fig.5), with the Bayesian method (as in Figs.10,11). Top: Energy range 2000 -2080 keV. Bottom: Energy range of analysis $\pm 4.4\sigma$ around $Q_{\beta\beta}$.

Comparison with Earlier Results

We applied the same methods of peak search as used in sections 3.3, 3.4, to the spectrum measured in the Ge experiment by Caldwell et al.[92] more than a decade ago. These authors had the most sensitive experiment using *natural* Ge detectors (7.8% abundance of ^{76}Ge). With their background being a factor of 9 higher than in the present experiment, and their measuring time of 22.6 kg y, they have a statistics for the background larger by a factor of almost 4 in their (very similar) experiment. This allows helpful conclusions about the nature of the background. The peak scanning finds [45,96] (Fig.16) indications for peaks essentially at the same energies as in Figs.10.11,12. This shows that these peaks are not fluctuations. In particular it sees the 2010.78, 2016.7, 2021.6 and 2052.94 keV ^{214}Bi lines. It finds, however, *no line at* $Q_{\beta\beta}$ (see also Fig.17). This is consistent with the expectation from the rate found from the HEIDELBERG-MOSCOW experiment. About 16 observed events in the latter correspond to 0.6 *expected* events in the Caldwell experiment, because of the use of non-enriched material and the shorter measuring time.

Another Ge experiment (IGEX) using 9 kg of enriched ^{76}Ge, but collecting since beginning of the experiment in the early nineties till shutdown in end of 1999 only 8.8 kg y of statistics[97], because of this low statistics also naturally cannot see any signal at 2039 keV. It sees, however, also the line around 2030 keV indicated in Figs.10,11,12 from our data.

Proofs and Disproofs

The result described in section 3 has been questioned in some papers (Aalseth et al, hep-ex/0202018; Feruglio et al., Nucl. Phys. B 637(2002) 345; Zdesenko et al., Phys. Lett. B 546(2002) 206, and Kirpichnikov, talk at Meeting of Physical Section of

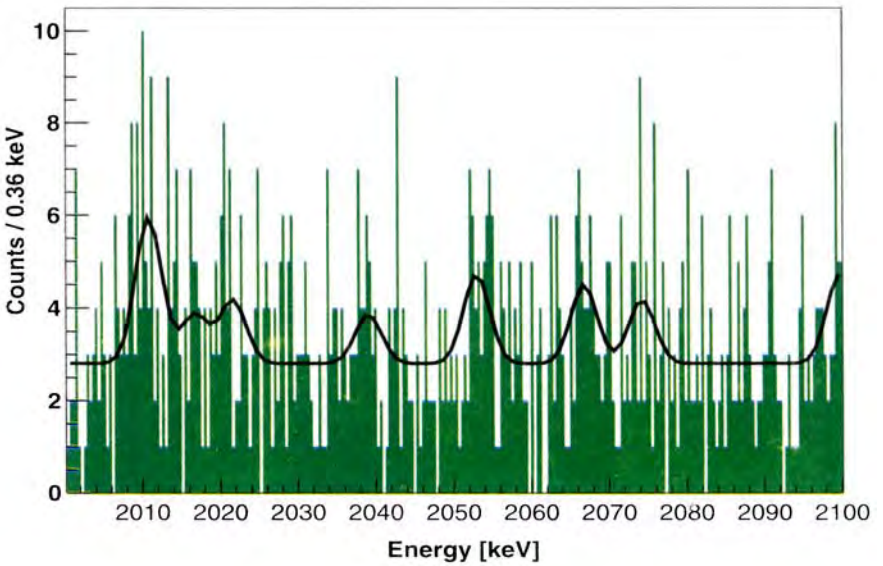

Fig. 13 Simultaneous analysis of the spectrum measured with the ^{76}Ge detectors Nr. 1,2,3,4,5 over the period August 1990 - May 2000 (54.9813 kg y) (same as in Fig.4, but here shown in the 0.36 keV original binning) in the energy range 2000 - 2060 keV, with the Maximum Likelihood Method. The probability for a line at 2039.0 keV found in this way is 91%.

Russian Academy of Sciences, Moscow, December 2, 2002, and priv. communication, Dec.3, 2002.) These claims against our results are incorrect in various ways.

The arguments in the first two of these papers can be easily rejected. We have published this in hep-ph/0205228. In particular their estimates of the intensities of the ^{214}Bi lines are simply wrong, because the summing effect of the energies of consecutive gamma lines (known as True Coincidence Summing - TCS in nuclear spectroscopy) was not taken into account (see Table VII in the present paper, and in ref.[45]). Further none of the papers have performed a Monte Carlo simulation of our setup, which is the only way to come to quantitative statements.

The paper by Zdesenko et al. starts from an arbitrary assumption, namely that there are lines in the spectrum *at best* only at 2010 and 2053 keV. This contradicts the experimental result, according to which there are further lines in the spectrum (see Figs.10,11,12,16 in the present paper). In this way they artificially increase the background in their analysis and come to wrong conclusions.

All three of these papers, when discussing the choice of the width of the search window, ignore the results of the statistical simulations we give in hep-ph/0205228 and we have published in refs.[44,45] (see also Fig.9 in the present paper).

Kirpichnikov states that from his analysis he clearly sees the 2039 keV line in the full (not pulse shape discriminated) spectrum with $> 99\%$ c.l. He claims that he does not see the signal in the pulse shape spectrum. One reason to see less intensity there certainly is that in this case he averages for determination of the background over the full energy range without allowing for any lines. His result is in contradiction with the result we obtain under the same assumption of assuming just one line (at $Q_{\beta\beta}$) and a continuous background (see Fig.12 of this paper).

4 Half-life of the Neutrinoless Mode and Effective Neutrino Mass

Having shown that the signal at $Q_{\beta\beta}$ consists of single site events and is not a γ line, we translate the observed number of events into half-lives for the neutrinoless double beta decay. We give in Table VIII conservatively the values obtained with the Bayesian method and not those obtained with the Feldman-Cousins method.

We derive from the data taken with 46.502 kg y the half-life $T^{0\nu}_{1/2} = (0.8 - 18.3) \times 10^{25}$ y (95% c.l.). The analysis of the other data sets, shown in Table VIII confirm this result. Of particular importance is that

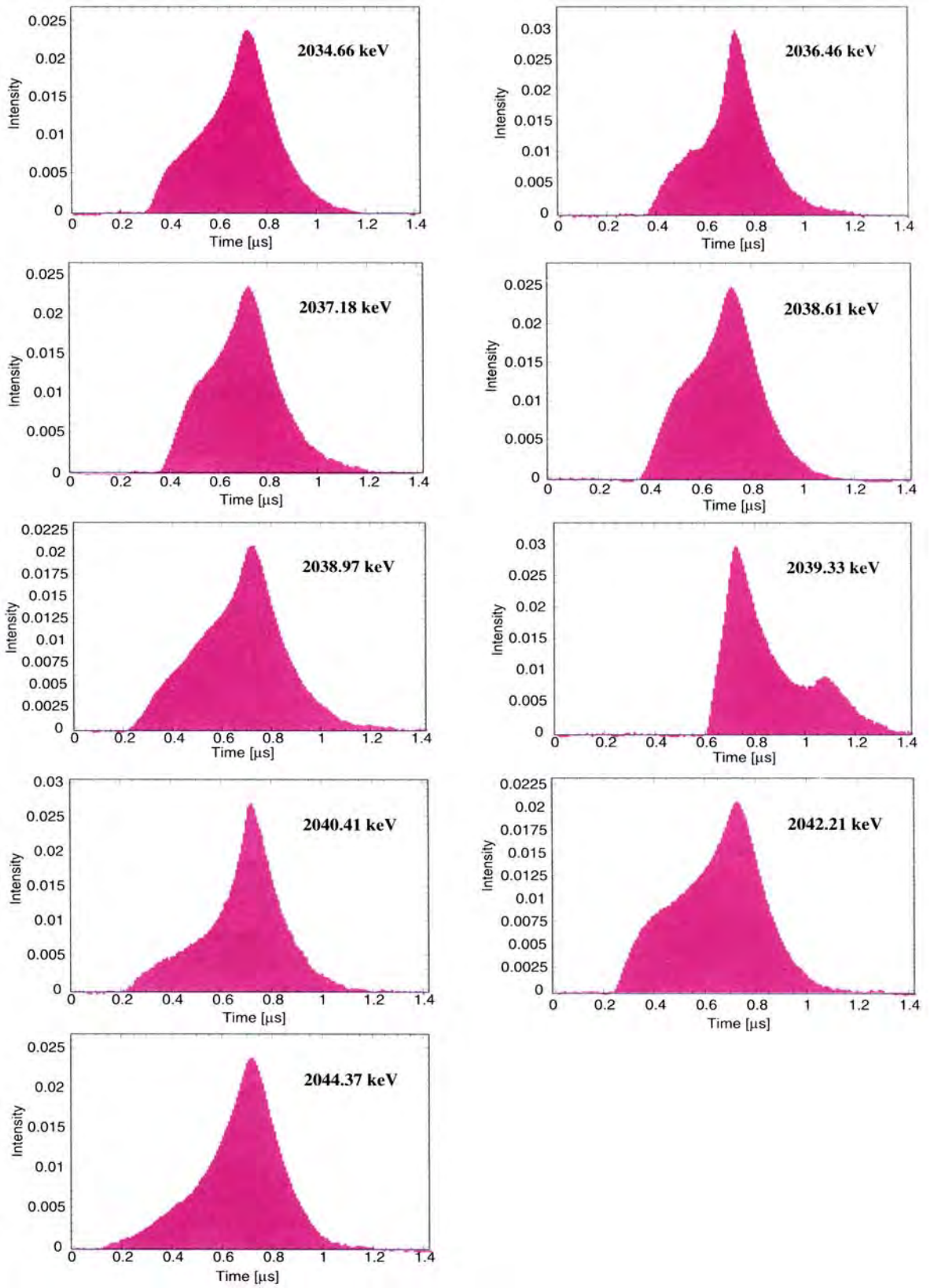

Fig. 14 Events classified to be single site events (SSE) by all three methods of PSA in the range 2034.1 - 2044.9 keV, in the measurement period 10.1995 - 05.2000, 28.053 kg y.

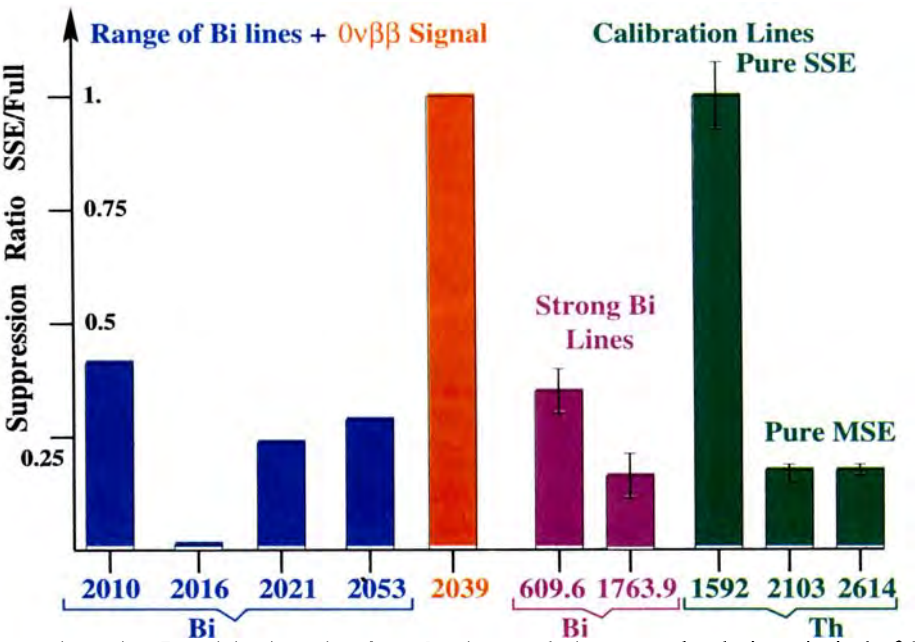

Fig. 15 Relative suppression ratios: Remaining intensity after pulse shape analysis compared to the intensity in the full spectrum. Right: Result of a calibration measurement with a Th source - ratio of the intensities of the 1592 keV line (double escape peak, known to be 100% SSE), set to 1. The intensities of the 2203 keV line (single escape peak, known to be 100% MSE) as well as of the 2614 keV line (full energy peak, known to be dominantly MSE) are strongly reduced (error bars are $\pm 1\sigma$). The same order of reduction is found for the strong Bi lines occurring in our spectrum (see Fig. 3) - shown in this figure are the lines at 609.4 and 1763.9 keV. Left: The lines in the range of weak statistics around the line at 2039 keV (shown are ratios of best fit values). The Bi lines are reduced compared to the line at 2039 keV (set to 1), as to the 1592 keV SSE Th line.

Table VIII

Half-life for the neutrinoless decay mode and deduced effective neutrino mass from the HEIDELBERG-MOSCOW experiment.

Significance [kg y]	Detectors	$T^{0\nu}_{1/2}$ y	$\langle m \rangle$ eV	Conf. level
54.9813	1,2,3,4,5	$(0.80 - 35.07) \times 10^{25}$	(0.08 - 0.54)	95% *c.l.*
		$(1.04 - 3.46) \times 10^{25}$	(0.26 - 0.47)	68% *c.l.*
		1.61×10^{25}	0.38	Best Value
46.502	1,2,3,5	$(0.75 - 18.33) \times 10^{25}$	(0.11 - 0.56)	95% *c.l.*
		$(0.98 - 3.05) \times 10^{25}$	(0.28 - 0.49)	68% *c.l.*
		1.50×10^{25}	0.39	Best Value
28.053	2,3,5 SSE	$(0.88 - 22.38) \times 10^{25}$	(0.10 - 0.51)	90% *c.l.*
		$(1.07 - 3.69) \times 10^{25}$	(0.25 - 0.47)	68% *c.l.*
		1.61×10^{25}	0.38	Best Value

Table IX

The effect of nuclear matrix elements on the deduced effective neutrino masses. Shown are the neutrino masses deduced from the best value of $T^{0\nu}_{1/2} = 1.5 \times 10^{25}$ y *determined in this work with 97% c.l. when using matrix elements from various calculations and a phase factor of* $F_1^{0\nu} = 6.31 \times 10^{-15}\,y^{-1}$

$M^{0\nu}$ from	104, 24	25	105	106	107	108	21	27, 28
$\langle m \rangle$ eV 95%	0.39	0.37	0.34	1.06	0.87	0.60	0.53	0.44 - 0.52

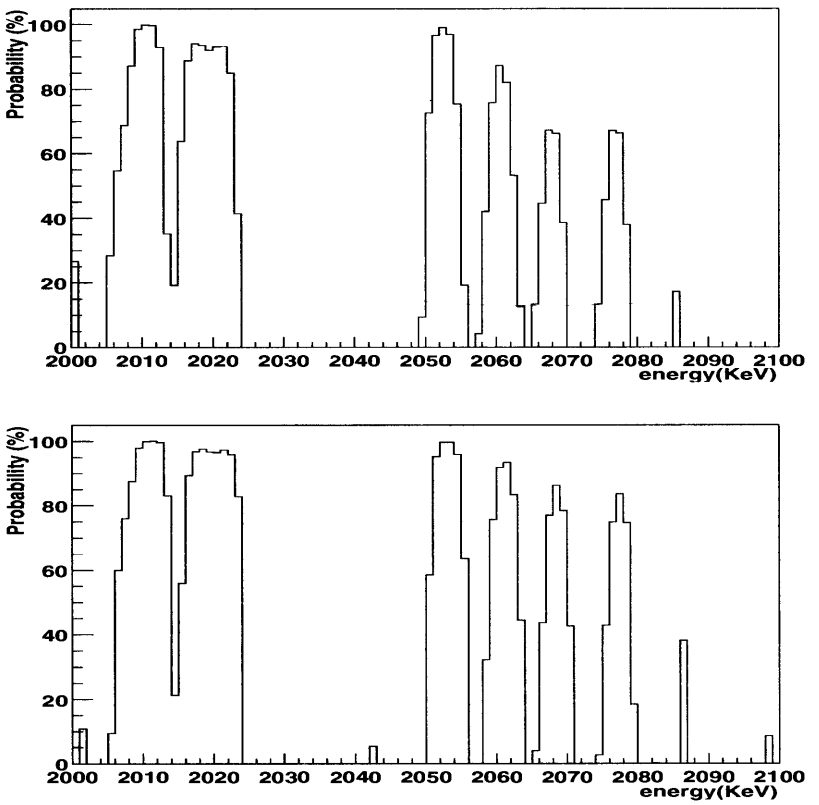

Fig. 16 Peak scanning of the spectrum measured by Caldwell et al.[92] with the Maximum Likelihood method (upper part), and with the Bayesian method (lower part) (as in Fig.10,11,12) (see ref.[74]).

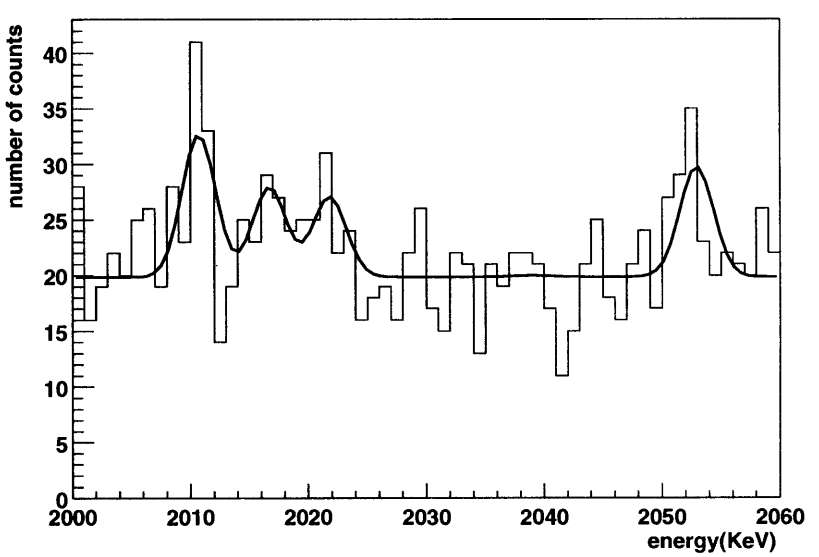

Fig. 17 Analysis of the spectrum measured by D. Caldwell et al.[92], with the Maximum Likelihood Method, in the energy range 2000 - 2060 keV (as in Fig.13) assuming lines at 2010.78, 2016.70, 2021.60, 2052.94, 2039.0 keV. In contrast to Fig.13 no indication for a signal at 2039 kev is observed (see text).

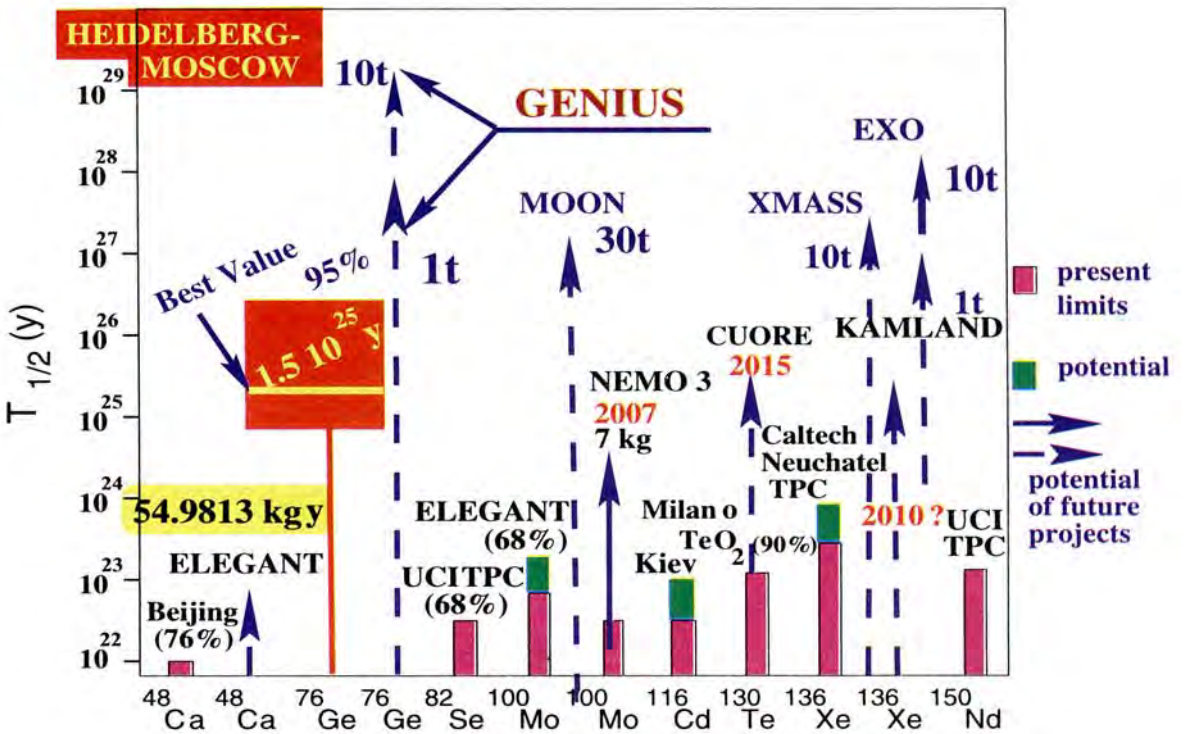

Fig. 18 Present evidence for $0\nu\beta\beta$ decay from data of the HEIDELBERG-MOSCOW experiment and the potential of present and future $\beta\beta$ experiments. Vertical axis - half life limits (only HEIDELBERG-MOSCOW gives a value) in years, horizontal - isotopes used in the various experiments.

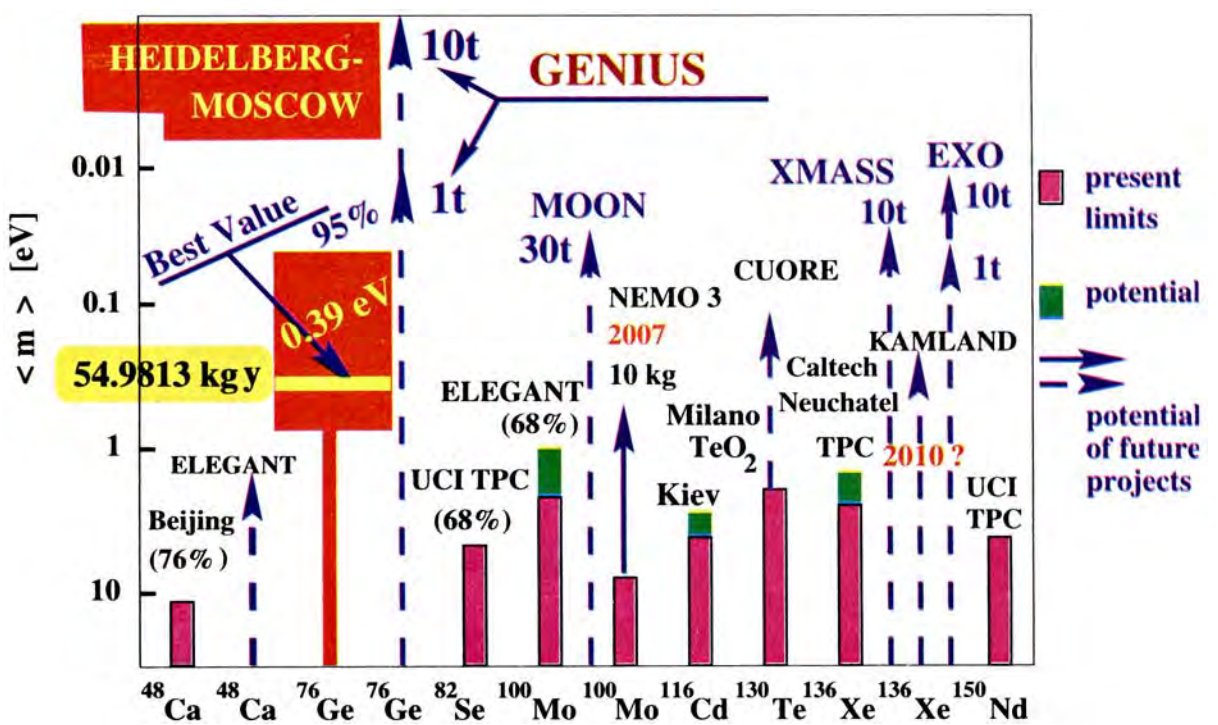

Fig. 19 Present evidence for $0\nu\beta\beta$ decay from data of the HEIDELBERG-MOSCOW experiment and the potential of present and future $\beta\beta$ experiments. Vertical axis - effective neutrino mass limits (only HEIDELBERG-MOSCOW gives a value) in eV, horizontal isotopes used in the various experiments.

we see the $0\nu\beta\beta$ signal in the single site spectrum.

The result obtained is consistent with the limits given by all other double beta experiments - which still reach less sensitivity (see Figs.18,19). The most sensitive experiments following the HEIDELBERG-MOSCOW experiment are the geochemical ^{128}Te experiment with $T^{0\nu}_{1/2} > 2(7.7) \times 10^{24}$ y (68% c.l.), [99] the ^{136}Xe experiment by the DAMA group with $T^{0\nu}_{1/2} > 1.2 \times 10^{24}$ y (90% c.l.)[100], a second ^{76}Ge experiment[101] with $T^{0\nu}_{1/2} > 1.2 \times 10^{24}$ y and a ^{nat}Ge experiment with[92,101] $T^{0\nu}_{1/2} > 1 \times 10^{24}$ y. Other experiments are already about a factor of 100 less sensitive concerning the $0\nu\beta\beta$ half-life: the Gotthard TPC experiment with ^{136}Xe yields[102] $T^{0\nu}_{1/2} > 4.4 \times 10^{23}$ y (90% c.l.) and the Milano Mibeta cryodetector experiment[103] $T^{0\nu}_{1/2} > 1.44 \times 10^{23}$ y (90% c.l.).

Another experiment[97] with enriched ^{76}Ge, which has stopped operation in 1999 after reaching a significance of 8.8 kg y, yields (if one believes their method of 'visual inspection' in their data analysis), in a conservative analysis, a limit of about $T^{0\nu}_{1/2} > 5 \times 10^{24}$ y (90% c.l.). The ^{128}Te geochemical experiment yields $\langle m_\nu \rangle < 1.1$ eV (68 % c.l.)[99], the DAMA ^{136}Xe experiment $\langle m_\nu \rangle < (1.1 - 2.9)$ eV[100] and the ^{130}Te cryogenic experiment yields $\langle m_\nu \rangle < 1.8$ eV[103].

Concluding we obtain, with more than 95% probability, first evidence for the neutrinoless double beta decay mode.

As a consequence, at this confidence level, lepton number is not conserved. Further our result implies that the neutrino is a Majorana particle. Both of these conclusions are *independent* of any discussion of nuclear matrix elements.

The matrix element enters when we derive - under the *assumption* that the $0\nu\beta\beta$ amplitude is dominated by the neutrino mass mechanism, a *value* for the effective neutrino mass. On using the nuclear matrix element from refs.[24,104], we conclude from the various analyses given above the effective mass $\langle m \rangle$ to be $\langle m \rangle$ = (0.11 - 0.56) eV (95% c.l.), with best value of 0.39 eV (see Table VIII). Allowing conservatively for an uncertainty of the nuclear matrix elements of $\pm$ 50% (for detailed discussions of the status of nuclear matrix elements we refer to refs.[7,14-15,21,25-28]) this range may widen to $\langle m \rangle$ = (0.05 - 0.84) eV (95% c.l.). In Table IX we demonstrate the situation of nuclear matrix elements by showing the neutrino masses deduced from different calculations (see ref.[45]). It should be noted that the value obtained in Large Scale Shell Model Calculations[106] is understood to be too large by almost a factor of 2 because of the too small configuration space, (see, e.g. ref.[26]), and that the second highest value given (from ref.[107]), has now been reduced[21] to 0.53 eV. The recent studies in refs.[27,28] yield an effective mass of (0.44 - 0.52) eV. We see that the early calculations[24] done in 1989 agree within less than 25% with the most recent values.

In the above conclusion for the effective neutrino mass, it is assumed that contributions to $0\nu\beta\beta$ decay from processes other than the exchange of a Majorana neutrino (see, e.g. refs.[7,109] and section 1) are negligible. It has been discussed, however, recently[54] that the possibility that $0\nu\beta\beta$ decay is caused by R-parity violation, may experimentally not be excluded, although this would require making R-parity violating couplings generation-dependent.

Assuming other mechanisms to dominate the $0\nu\beta\beta$ decay amplitude, the result allows to set stringent limits on parameters of SUSY models, leptoquarks, compositeness, masses of heavy neutrinos, the right-handed W boson and possible violation of Lorentz invariance and equivalence principle in the neutrino sector. For a discussion and for references we refer to refs.[7,20,40,110,111].

5 Consequences

With the value deduced for the effective neutrino mass, the HEIDELBERG-MOSCOW experiment excludes several of the neutrino mass scenarios allowed from present neutrino oscillation experiments (see Fig.20) - allowing only for degenerate mass scenarios, and an inverse hierarchy 3ν and 4ν- scenario. For details we refer to ref.[5]. In particular, hierarchical mass schemes are excluded at the present level of accuracy.

According to a global analysis[2] all solar neutrino data including the recent SNO neutral-current rate selects the Large Mixing Angle (LMA) at the 90% c.l.; however, the LOW solution is also viable, with 0.89 goodness of fit. Recently the LMA solution has been supported by evidence for reactor antineutrino disappearance[3].

Assuming the degenerate scenario to be realized in nature we fix–according to the formulae derived in ref.[6]–the common mass eigenvalue of the degenerate neutrinos to m = (0.05 - 3.4) eV. Part of the up-

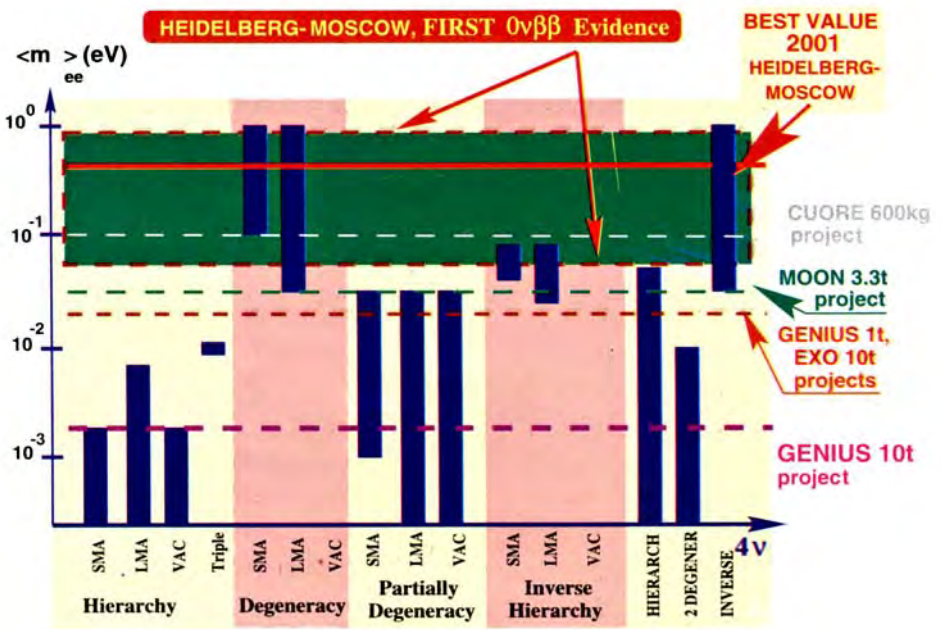

Fig. 20 The impact of the evidence obtained for neutrinoless double beta decay in this paper (best value of the effective neutrino mass $\langle m \rangle$ = 0.39 eV, 95% confidence range (0.05 - 0.84) eV - allowing already for an uncertainty of the nuclear matrix element of a factor of ± 50%) on possible neutrino mass schemes. The bars denote allowed ranges of $\langle m \rangle$ in different neutrino mass scenarios, still allowed by neutrino oscillation experiments. Hierarchical models are excluded by the new $0\nu\beta\beta$ decay result. Also shown are the expected sensitivities for the future potential double beta experiments CUORE, MOON, EXO and the 1 ton and 10 ton project of GENIUS[98] (from ref.[5]).

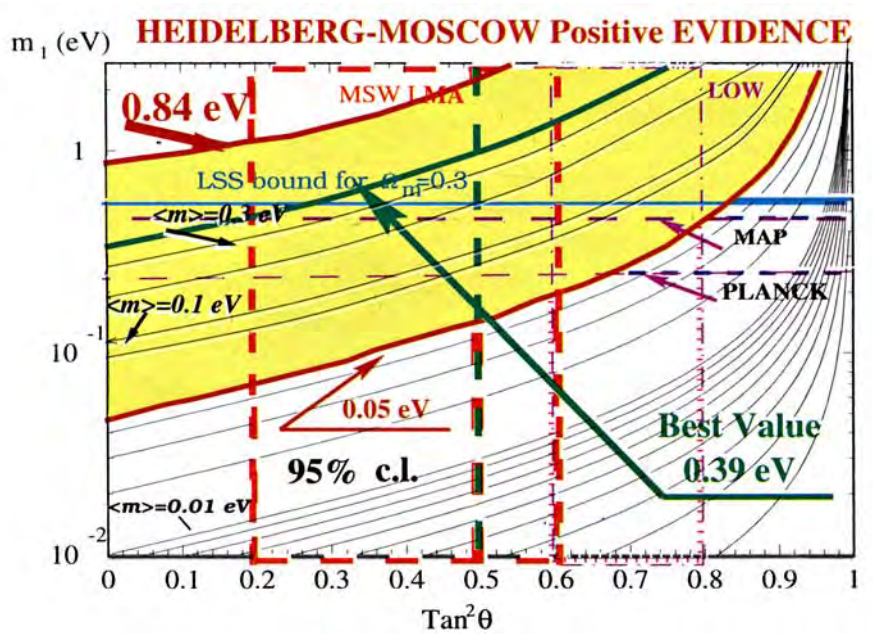

Fig. 21 Double beta decay observable $\langle m \rangle$ and oscillation parameters: The case for degenerate neutrinos. Plotted on the axes are the overall scale of neutrino masses m_0 and mixing $\tan^2 \theta_{12}$. Also shown is a cosmological bound deduced from a fit of CMB and large scale structure[112] and the expected sensitivity of the satellite experiments MAP and PLANCK. The present limit from tritium β decay of 2.2 eV[113] would lie near the top of the figure. The range of $\langle m \rangle$ fixed by the HEIDELBERG-MOSCOW experiment is, in the case of small solar neutrino mixing, already in the range to be explored by MAP and PLANCK.

per range is already excluded by tritium experiments, which give a limit of m < 2.2 eV, or 2.8 eV (95% c.l.)[113]. The full range can only partly (down to ~ 0.5 eV) be checked by future tritium decay experiments, but could be checked by some future $\beta\beta$ experiments (see, e.g. refs.[7,98,114]). The deduced 95% interval for the sum of the degenerate neutrino masses is consistent with the range for Ω_ν deduced from recent cosmic microwave background measurements and large scale structure (redshift) surveys, which still allow for a $\sum_i m_i \leq 4.4\,\mathrm{eV}$[115,116]. The range of $\langle m \rangle$ fixed in this work is, already now, in the range to be explored by the satellite experiments MAP and PLANCK[112,46] (see Fig.21). It lies in a range of interest for Z-burst models recently discussed as explanation for super-high energy cosmic ray events beyond the GKZ-cutoff[65,117,118]. Finally, the deduced best value for the mass is consistent with expectations from experimental $\mu \rightarrow e\gamma$ branching limits in models assuming the generating mechanism for the neutrino mass to be also responsible for the recent indication for an anomalous magnetic moment of the muon[119]. A recent model with underlying A_4 symmetry for the neutrino mixing matrix (and the quark mixing matrix) also leads to degenerate neutrino masses consistent with the present experiment[120]. This model succeeds to consistently describe the large (small) mixing in the neutrino (quark) sector.

The neutrino mass deduced leads to $0.002 \leq \Omega_\nu h^2 \leq 0.1$, and thus may allow neutrinos to still play an important role as hot dark matter in the Universe (see also refs.[53,121]).

6 Future of $\beta\beta$ Experiments - GENIUS and Other Proposals

With the HEIDELBERG-MOSCOW experiment, the era of the small smart experiments is over. New approaches and considerably enlarged experiments (as discussed in refs.[7,19,98,114,122]) will be required in future to fix the neutrino mass with higher accuracy.

Since it was realized in the HEIDELBERG-MOSCOW experiment, that the remaining small background is coming from the material close to the detector (holder, copper cap, ...), elimination of *any* material close to the detector will be decisive. Experiments which do not take this into account, like, e.g. CUORE[103,123], and MAJORANA[124], will allow only rather limited steps in sensitivity.

Further there is the problem in cryodetectors that they cannot differentiate between a β and γ signal, as is possible in Ge experiments. Another crucial point is–see eq. (6)–the energy resolution, which can be optimized *only* in experiments using Germanium detectors or bolometers. It will be difficult to probe evidence for this rare decay mode in experiments, which have to work–as a result of their limited resolution–with energy windows around $Q_{\beta\beta}$ of up to several hundreds of keV, such as NEMO III[125], EXO[126] and CAMEO[127].

Another important point is (see eq. 6), the efficiency of a detector for detection of a $\beta\beta$ signal. For example, with 14% efficiency, a potential future 100 kg ^{82}Se NEMO experiment would be equivalent only to a 10 kg experiment (not talking about the energy resolution).

In the first proposal for a third generation double beta experiment, the GENIUS proposal[40,98,?], the idea is to use 'naked' Germanium detectors in a huge tank of liquid nitrogen. It seems to be at present the *only* proposal which can fulfill *both* requirements mentioned, namely, to increase the detector mass and to simultaneously reduce the background drastically. The potential of GENIUS together with that of some later proposals is indicated in Fig.20. GENIUS would–with only 100 kg of enriched ^{76}Ge–increase the confidence level of the present pulse shape discriminated signal to 4σ within one year, and to 7σ within 3 years of measurement (a confirmation on a 4σ level by the MAJORANA project would need ~ 230 years, while the CUORE project would need (ignoring the problem of identification of the signal as $\beta\beta$ signal) 3700 years). With ten tons of ^{76}Ge GENIUS should be capable to investigate also, whether the neutrino mass mechanism or another mechanism (see, e.g. ref.[7]) is dominating the decay amplitude. A GENIUS Test Facility is at present under construction in the GRAN SASSO Underground Laboratory[128,129].

7 Conclusion

The status of present double beta decay search has been presented, and recent evidence for a non-vanishing Majorana neutrino mass obtained by the HEIDELBERG-MOSCOW experiment about one year ago has been described and outlined. Future projects to improve the present accuracy of the effec-

8 Acknowledgments

The author is indebted to his colleaques A. Dietz and I.V. Krivosheina for the fruitful and pleasant collaboration, and to C. Tomei and C. Dörr for their help in the analysis of the Bi lines.

References

1 J H Bahcall, M C Gonzalez-Garcia and C Pena-Garay *hep-ph/*0106258 and CERN-TH/2001–165

2 V Barger *et al Phys Lett* B **537** (2002) 179–186 and *hep-ph/*0204253

3 K Eguchi *et al* subm to *Phys Rev Lett* 6 December 2002

4 M H Ahn *et al* hep-ex/0212007

5 H V Klapdor-Kleingrothaus and U Sarkar *Modern Physics Letters* A **16** 2469-2482 (2001) 38

6 H V Klapdor-Kleingrothaus, H Päs and A Yu Smirnov *Phys Rev* D **63** (2001) 073005 and hep-ph/0003219 (2000) and hep-ph/0103076 (2001) and in Proc of 3rd International Conference on Dark Matter in Astro and Particle Physics (Dark 2000) Heidelberg, Germany, 10-16 July 2000 ed: H V Klapdor-Kleingrothaus Springer, Heidelberg (2001) 420

7 H V Klapdor-Kleingrothaus *60 Years of Double Beta Decay - From Nuclear Physics to Beyond the Standard Model* World Scientific, Singapore (2001) 1281 pp

8 E Majorana *Nuovo Cimento* **14** (1937) 171

9 G Racah *Nuovo Cimento* **14** (1937) 322

10 J A Mclennan *Jr Phys Rev* **106** (1957) 821

11 K M Case *Phys Rev* **107** (1957) 307

12 D V Ahluwalia *Int J Mod Phys* A **11** (1996) 1855

13 M Doi, T Kotani and E Takasugi *Prog of Theor Phys Suppl* **83** (1985) 1

14 K Muto and H V Klapdor in *Neutrinos, Graduate Texts in Contemporary Physics* ed: H V Klapdor Berlin Germany Springer (1988) 183

15 K Grotz and H V Klapdor *Die Schwache Wechselwirkung in Kern- Teilchen-und Astrophysik*; B G Teubner Stuttgart (1989); *The Weak Interaction in Nuclear Particle and Astrophysics* IOP Bristol (1990) Moscow MIR (1992) and China (1998)

16 H V Klapdor-Kleingrothaus and A Staudt *Teilchenphysik ohne Beschleuniger* B G Teubner Stuttgart (1995) *Non-Accelerator Particle Physics* IOP Publishing Bristol and Philadelphia (1995) and 2 ed (1998) and Moscow Nauka Fizmalit (1998) translated by V A Bednyakov

17 W H Furry *Phys Rev* **56** (1939) 1184

18 H Päs, M Hirsch, H V Klapdor-Kleingrothaus and S G Kovalenko *Phys Lett* **B 453** (1999) 194

19 H V Klapdor-Kleingrothaus *Int J Mod Phys* A **13** (1998) 3953 and in Proc of Int Symposium on Lepton and Baryon Number Violation, Trento Italy 20–25 April 1998 ed: H V Klapdor-Kleingrothaus and I V Krivosheina *IOP Bristol* (1999) 251 and *Preprint hep-ex/*9901021

20 H V Klapdor-Kleingrothaus *Springer Tracts in Modern Physics* **163** (2000) 69 *Springer-Verlag Heidelberg Germany* (2000)

21 F Simkovic *et al Phys Rev* C **64** (2001) 035501

22 J Schechter and J W F Valle *Phys Rev* D **25** (1982) 2951

23 M Hirsch and H V Klapdor-Kleingrothaus *Phys Lett* B **398** (1997) 311; *Phys Rev* D **57** (1998) 1947; M Hirsch, H V Klapdor-Kleingrothaus and St Kolb *Phys Rev* D **57** (1998) 2020

24 A Staudt, K Muto and H V Klapdor Kleingrothaus *Eur Phys Lett* **13** (1990) 31

25 T Tomoda *Rept Prog Phys* **54** (1991) 53

26 A Faessler and F Simkovic *J Phys* G **24** (1998) 2139

27 S Stoica and H V Klapdor-Kleingrothaus *Nucl Phys* A **694** (2001) 269

28 S Stoica and H V Klapdor-Kleingrothaus *Phys Rev* C **63** (2001) 064304

29 HEIDELBERG-MOSCOW Collaboration *Phys Lett* B **407** (1997) 219

30 HEIDELBERG-MOSCOW Collaboration *Phys Rev Lett* **83** (1999) 41

31 H V Klapdor-Kleingrothaus *et al* (HEIDELBERGMOSCOW Collaboration) *Eur Phys J* A **12** (2001) 147 and hep-ph/0103062 in Proc of Third International Conference on Dark Matter in Astro- and Particle Physics, DARK2000; H V Klapdor-Kleingrothaus (Editor) Springer-Verlag Heidelberg (2001) 520

32 H Georgi und S L Glashow *Phys Rev* D **61** (2000) 097301 and hep-ph/9808293

33 J Ellis and S Lola *Phys Lett* B **458** (1999) 310 and *hep-ph/* 9904279

34 R Adhikari and G Rajasekaran *Phys Rev* D **61** (1999) 031301(R)

35 H Minakata and H Nunokawa *Phys Lett* B **504** (2001) 301 and *hep-ph/* 0010240

36 H Minakata in *hep-ph/*0101148

37 H Minakata and O Yasuda *Phys Rev* D **56** (1997) 1692 and *hep-ph/* 9609276

38 H V Klapdor Vorschlag eines Experiments *Internal Report* MPI H V **17** (1987) 18pp

39 M Günther *et al* HEIDELBERG-MOSCOW Collaboration *Phys Rev* D **55** (1997) 54

40 H V Klapdor-Kleingrothaus in Proc of 18th Int Conf on NEUTRINO 98 Takayama Japan 4–9 Jun 1998 eds: Y Suzuki *et al Nucl Phys Proc Suppl* **77** (1999) 357

41 H V Klapdor-Kleingrothaus in Proc of the 17th International Conference Neutrino Physics and Astrophysics NEUTRINO 96 Helsinki Finland June (1996) 13 eds: K Enqvist, K Huitu and J Maalampi *World Scientific Singapore* (1997) 317

42 H V Klapdor-Kleingrothaus in Proc of the Int Symposium on Advances in Nuclear Physics eds; D Poenaru and S Stoica *World Scientific Singapore* (2000) 123

43 H V Klapdor-Kleingrothaus, A Dietz, H V Harney and I V Krivosheina *Modern Physics Letters* A **16** No 37 (2001) 2409 and *hep-ph/* 0201231

44 H V Klapdor-Kleingrothaus *et al Part and Nucl Lett* **110** No 1 (2002) 57; and in Proc of BEYOND 2002 Oulu Finland June 2002 eds: (IOP Bristol and Philadelphia 2002) eds: H V Klapdor-Kleingrothaus *et al*; H V Klapdor-Kleingrothaus *et al* to be publ (2002)

45 H V Klapdor-Kleingrothaus *et al Found of Phys* **32** No 8 (2002) 1181

46 H V Klapdor-Kleingrothaus in Proc of Intern Conf Flavor Physics ICFP01 31 May June 2001 Zhang-Jia-jie China ed by Y-L Wu *World Scientific Singapure* (2002) 93

47 H V Klapdor-Kleingrothaus in Proc of Intern Conf Zacatecas Forum in Physics 2002 11–13 May 2002 Zacatecas Mexico Found of Physics 2003 eds: D Ahluwalia and M Kirchbach

48 H V Klapdor-Kleingrothaus in Proc of Fourth Intern Heidelberg Conf on DARK MATTER IN ASTRO AND PARTICLE PHYSICS (DARK 2002) February 4–9 2002 Cape Town South Africa Springer Heidelberg 2002 eds: H V Klapdor Kleingrothaus and R D Viollier

49 H V Klapdor-Kleingrothaus in Proc of Third International Conference on Physics Beyond the Standard Model "Accelerator Non-Accelerator and Space Approaches" (BEYOND THE DESERT 02) June 2–7 2002 Oulu Finland IOP Bristol 2003 ed: H V Klapdor-Kleingrothaus

50 H V Klapdor-Kleingrothaus in Proc of Intern Conf " Neutrinos and Implications for Physics Beyond the Standard Model" Stony Brook October 11–13 2002

51 H V Klapdor-Kleingrothaus and U Sarkar to be publ *Phys Lett* B (2002) and *hep-ph/*0201226 and *Phys Lett* B **532** (2002) 71 and *hep-ph/*0202006

52 E Ma *Mod Phys Lett* A **17** (2002) 289 and *hep-ph/*0201225

53 V Barger, S L Glashow, D Marfatia and K Whisnant *Phys Lett* B **532** (2002) 15 and *hep-ph/*0201262

54 Y Uehara *Phys Lett* B **537** (2002) 256 *hep-ph/* 0201277; *hep-ph/* 0205294

55 H Minakata and H Sugiyama *Phys Lett* B **532** (2002) 275 and *hep-ph/*0202003

56 U Chattopadhyay *et al hep-ph/*0201001

57 Zhi-zhong Xing *Phys Rev* D **65** (2002) 077302 and *hep-ph/*0202034

58 T Hambye *hep-ph/*0201307

59 D V Ahluwalia and M Kirchbach *hep-ph/* 0204144 and to be publ *Phys Lett* B (2002); *Phys Lett* B **529** (2002) 124 and *hep-th/*0202164; and *gr-qc/***0207004**

60 E Witten *Nature* **415** (2002) 969

61 B Brahmachari and E Ma *Phys Lett* B **536** (2002) 259 and *hep-ph/*0202262

62 N Haba and T Suzuki *Mod Phys Lett* A **17** (2002) 865 and *hep-ph/*0202143; and *hep-ph/*0205141

63 B Brahmachari, S Choubey and R N Mohapatra *Phys Lett* B **536** (2002) 94 and *hep-ph/*0204073

64 G Barenboim *et al Phys Lett* B **537** (2002) 227 and *hep-ph/*0203261

65 Z Fodor, S D Katz and A Ringwald *JHEP* **0206** (2002) 046 and *hep-ph/*0203198

66 S Pakvasa and P Roy *Phys Lett* B **535** (2002) 181 and *hep-ph/*0203188

67 H B Nielsen and Y Takanishi *hep-ph/*0110125 and *Nucl Phys* B **636** (2002) 305 and *hep-ph/*0204027

68 D A Dicus, H-J He and J N Ng *Phys Lett* B **537** (2002) 83 and *hep-ph/*0203237

69 A S Joshipura and S D Rindani *hep-ph/*0202064

70 G C Branco *et al hep-ph/*0202030

71 M-Y Cheng and K Cheung *hep-ph/*0203051

72 M Frigerio and A Yu Smirnov *hep-ph/*0202247

73 K Matsuda *et al hep-ph/*0204254

74 H V Klapdor-Kleingrothaus *et al* to be publ (2002)

75 B Maier Dipl Thesis Univ Heidelberg 1993 and Dissertation November 1995 MPI-Heidelberg; F Petry Dissertation November 1995 MPI Heidelberg; J Hellmig Dissertation November 1996 MPI-Heidelberg; B Majorovits Dissertation December 2000 MPI-Heidelberg; A. Dietz Dipl Thesis Univ Heidelberg 2000 (unpublished) and Dissertation in preparation

76 G Douysset *et al Phys Rev Lett* **86** (2001) 4259

77 J G Hykawy *et al Phys Rev Lett* **67** (1991) 1708

78 R B Firestone and V S Shirley *Table of Isotopes* Eighth Edition John Wiley and Sons Incorp NY (1998) and S Y F Chu, L P Ekström and R B Firestone The Lund/LBNL Nuclear Data Search Vers 2.0 Febr 1999 and http:// nucleardata.nuclear.lu.se/nucleardata/toi/radSearch.asp

79 H V Klapdor-Kleingrothaus *hep-ph/*0205228

80 C M Baglin, S Y F Chu and J Zipkin *Table of isotopes* eight edition J Wiley & Sons Inc (1996)

81 W Struve *Nucl Phys* **222** (1973) 605

82 F Areodo *Il Nuovo Cimento* A **112** (1999) 819

83 H Liljavirta *Phycica Scripta* **18** (1978) 75

84 J Hellmig and H V Klapdor Kleingrothaus *Nucl Instrum Meth* A **455** (2000) 638

85 J Hellmig, F Petry and H V Klapdor-Kleingrothaus *Patent* **DE19721323A**

86 B Majorovits and H V Klapdor-Kleingrothaus. *Eur Phys J* A **6** (1999) 463

87 H V Klapdor-Kleingrothaus *et al* (HEIDELBERG-MOSCOW Collaboration) *Erratum Eur Phys J* (2002)

88 G D'Agostini hep-ex/0002055 W von der Linden and V Dose *Phys Rev* E **59** (1999) 6527 and F H Fröhner JEFF Report **18** NEA OECD (2000) and *Nucl Sci a Engineering* **126** (1997) 1

89 D E Groom *et al* Particle Data Group *Eur Phys J* C **15** (2000) 1

90 A O'Hagan "Bayesian Inference" B **2** of Kendall's Advanced Theory of Statistics Arnold London (1994)

91 A Dietz Dissertation (2003) MPI-Heidelberg

92 D Caldwell *J Phys G* **17** (1991) S137-S144

93 G J Feldman, R D Cousins *Phys Rev* D **57** (1998) 3873

94 http://root.cern.ch/

95 http://www.info.cern.ch/asd/lhc++/indexold.html

96 H V Klapdor-Kleingrothaus *et al* to be publ (2003)

97 C E Aalseth *et al* (IGEX Collaboration) *Yad Fiz* **63** 7 (2000) 1299; *Phys Rev* D **65** (2002) 092007

98 H V Klapdor-Kleingrothaus *hep-ph/*0103074 and in Proc of 2nd Workshop on Neutrino Oscillations and Their Origin (NOON 2000) Tokyo Japan 6-18 Dec 2000 ed; Y Suzuki *et al* World Scientific (2001);

H V Klapdor-Kleingrothaus *Nucl Phys Proc Suppl* **100** (2001) 309 and *hep-ph/* 0102276;

H V Klapdor-Kleingrothaus *Part Nucl Lett* **104** (2001) 20 and *hep-ph/* 0102319;

H V Klapdor-Kleingrothaus in Proceedings of BEYOND'97 First International Conference on Particle Physics Beyond the Standard Model Castle Ringberg Germany 8-14 June 1997 edited by H V Klapdor-Kleingrothaus and H Päs *IOP Bristol* (1998) 485;

H V Klapdor-Kleingrothaus *et al* MPI Report MPI-H-V26-1999 and Preprint *hep-ph/*9910205 and in Proceedings of the 2nd Int Conf on Particle Physics Beyond the Standard Model BEYOND'99 Castle Ringberg Germany 6–12 June 1999 edited by H V Klapdor-Kleingrothaus and I V Krivosheina *IOP Bristol* (2000) 915;

H V Klapdor-Kleingrothaus *Nucl Phys* **B 110** (2002) 58 Proc of TAUP'01 (2002) Gran-Sasso Italy September 7–13 2001 eds: A Bettini *et al*

99 O Manuel *et al* in Proc Intern Conf on Nuclear Beta Decays and the neutrinos eds: T Kotani *et al* WS (1986) 71 *J Phys G Nucl Part Phys* **17** (1991) S221-S229

100 R Bernabei *et al Phys Lett* (2002) 23

101 A A Vasenko, I V Kirpichnikov *et al Mod Phys Lett* A **5** (1990) 1299 and J G Hykaury *et al Phys Rev Lett* **67** (1991) 1708

102 R Luscher *et al Phys Lett* (1998) 407

103 (CUORE Coll) talk given on ApPEC Astroparticle Physics European Coordination Paris France 22.01.2002; A Alessandrello *et al Phys Lett* B **486** (2000) 13 and S Pirro *et al Nucl Instr Methods* A **444** (2000) 71

104 K Muto, E Bender and H V Klapdor *Z Phys* A **334** (1989) 177

105 W C Haxton and G J Stephenson *Prog Part Nucl Phys* **12** (1984) 409

106 E Caurier, F Nowacki, A Poves and J Retamosa *Phys Rev Lett* **77** (1996) 1954

107 F Šimkovic *et al Phys Lett* B **393** (1997) 267

108 F Šimkovic, G Pantis, J D Vergados and A Faessler *Phys Rev* C **60** (1999) 055502

109 R N Mohapatra and P B Pal "Massive Neutrinos in Physics and Astrophysics" Singapore *Singapore World Scientific* World Scientific lecture notes in physics **41** (1991) 318 pp

110 H V Klapdor-Kleingrothaus in Proceedings of BEYOND'97 First International Conference on Particle Physics Beyond the Standard Model Castle Ringberg Germany 8–14 June 1997 edited by H V Klapdor-Kleingrothaus and H Päs *IOP Bristol* (1998) 485 and in *Int J Mod Phys* A **13** (1998) 3953

111 H V Klapdor-Kleingrothaus in Proc of NANPino 2000 Dubna July 19–22 2000 *Particles and Nuclei Letters* **104 iss. 1/2** (2001) 20 and *hep-ph/* 0102319

112 R E Lopez *astro-ph/***9909414**; J R Primack and M A K Gross *astro-ph/***0007165**; J R Primack *astro-ph/***0007187**; J Einasto in Proc of DARK2000 Heidelberg Germany July 10–15 2000 ed: H V Klapdor-Kleingrothaus *Springer Heidelberg* (2001) 3

113 C Weinheimer in Proc of 3rd International Conference on Dark Matter in Astro and Particle Physics (Dark 2000) Heidelberg Germany 10–16 July 2000 ed: H V Klapdor-Kleingrothaus Springer Heidelberg (2001) 513

114 H V Klapdor-Kleingrothaus, J Hellmig and M Hirsch *J Phys* G **24** (1998) 483

115 M Tegmark *et al hep-ph/*0008145

116 X Wang, M Tegmark and M Zaldarriaga *Phys Rev* D **65** (2002) 123001 and *astro-ph/* **0105091**

117 D Fargion *et al* in Proc of DARK2000 Heidelberg Germany July 10–15 2000 ed: H V Klapdor Kleingrothaus *Springer Heidelberg* (2001) 455

118 T J Weiler in Proc Beyond the Desert 1999 Accelerator Non-Accelerator and Space Approaches Ringberg Castle Tegernsee Germany 6–12 June 1999 edited by H V Klapdor Kleingrothaus and I V Krivosheina IOP Bristol (2000) 1085; H Päs and T J Weiler *Phys Rev* D **63** (2001) 113015 and *hep-ph/*0101091

119 E Ma and M Raidal Phys Rev Lett **87** (2001) 011802; Erratum-ibid **87** (2001) 159901 and hep-ph/0102255

120 K S Babu, E Ma and J W F Valle hep-ph/0206292 v 1

121 H V Klapdor-Kleingrothaus *Int J Mod Phys* A **17** (2002) 3421 in Proc of Intern Conf LP01 Rome Italy July 2001

122 H V Klapdor-Kleingrothaus *Part Nucl Lett* **104** No 1 (2001) 20 and H V Klapdor-Kleingrothaus *Nucl Phys* B **110** (2002) 364 Proc of TAUP'01 (2002) Gran-Sasso Italy September 7–13 2001 ed: A Bettini *et al*

123 A Giuliani *et al Nucl Phys Proc Suppl* **110** (2002) 64

124 L DeBraekeleer talk at Worksh on the Next Generation US Underground Science Facility WIPP June 12–14 2000 Carlsbad New Mexico USA C E Aalseth *et al* Proc Taup 2001 Gran Sasso Italy 8–12 Sept 2001 (editors A Bettini *et al*)

125 X Sarazin (for the NEMO Collaboration) talk given on ApPEC Astroparticle Physics European Coordination Paris France Jan 22 2002; (NEMO Collaboration) Contr paper for XIX Int Conf NEUTRINO 2000 Sudbury Canada June 16–21 2000 LAL 00-31 (2000) 1 and (NEMO-III Collaboration) in Proc of NANPino2000 Dubna Russia July 2000 ed: V Bednjakov *Part and Nucl Lett* **3** 62 (2001)

126 G Gratta talk given on ApPEC Astroparticle Physics European Coordination Paris France Jan 22 2002 and in Proc of LowNu2 Dec 4–5 (2000) Tokyo Japan ed: Y Suzuki World Scientific (2001) p98

127 CAMEO Collaboration in Proc of Taup 2001 Gran Sasso Italy 8–12 Sept 2001 (editors A Bettini *et al*)

128 H V Klapdor-Kleingrothaus *et al Nucl Instr Meth* A **481** (2002) 149

129 T Kihm, V Bobrakov and H V Klapdor Kleingrothaus subm for publ 2002

130 H V Klapdor-Kleingrothaus in Proc of Int. Conference NOW2000 - "Origins of Neutrino Oscillations" ed: G Fogli *Nucl Phys* B **100** (2001) 309

131 V A Bednyakov and H V Klapdor Kleingrothaus *hep-ph/*0011233 and *Phys Rev* D **63** (2001) 095005

132 H V Klapdor-Kleingrothaus in Proc Int Workshop on Low Energy Solar Neutrinos LowNu2 Dec 4–5 ed: Y Suzuki *et al World Scientific Singapore* (2001)

133 T Bernatowicz, R Cowsik, C Hohenberg and F Podosek *Phys Rev Lett* **69** (1992) 2341 and *Phys Rev* C **47** (1993) 806